Stockholm University

# Bachelor Thesis

**Degree Project in Marine Geology 15 hp**

## Acoustic survey of sea floor features in Asköfjärden

Kim Lundmark

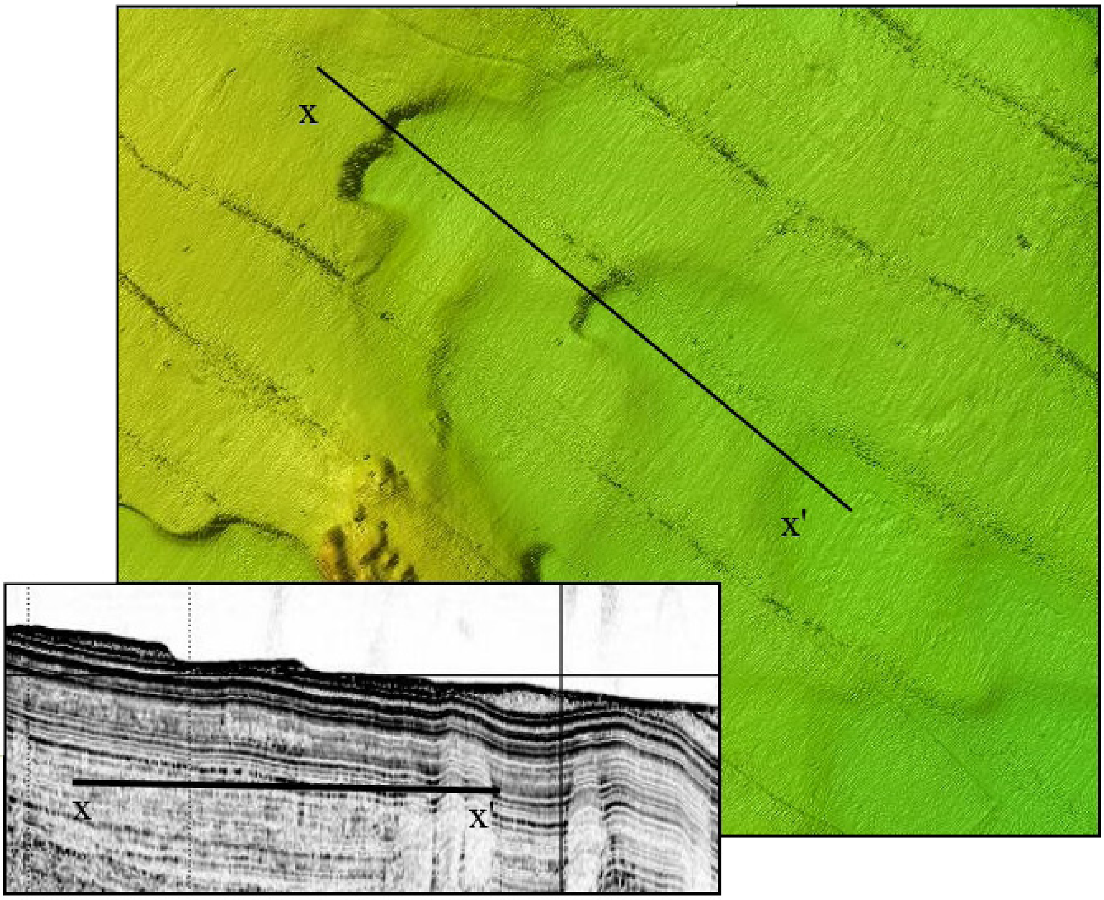


Stockholm 2017

Department of Geological Sciences
Stockholm University
SE-106 91 Stockholm
Sweden

## Sammanfattning
Maringeologiska undersökningar i Asköfjärden i Stockholms södra skärgård har påvisat trappstegsliknande objekt i sedimenten på Östersjöns botten. I detta projekt är målet att analysera trappstegen och undersöka bildningsmekanismer genom data från undersökningarna. I studien används de akustiska instrumenten multibeam-ekolod och Chirp sonar. Multibeam visar bottentopografin och kan också visa objekt i vattenkolumnen medan Chirp sonar visar sedimentlagren några tiotals meter ned i havsbotten. Multibeam visar flera halvmåneformade trappsteg samt elliptiska ”pockmarks”. Vattenkolumnsdata visar läckor från havsbotten under trappstegen och pockmarks. Sedimentprofilerna visar att bildandet av trappstegsformerna kan bero på antingen gas eller en annan fluid, som kan vara grundvatten. Ingen slutgiltig slutsats om trappstegens bildningsprocess kan göras på dataunderlaget i denna studie och det föreslås att petrofysiska och geokemiska undersökningar utförs som kan komplettera denna studie.

## Abstract
Marine geological surveys in Asköfjärden in the southern Stockholm Archipelago has revealed step like features in the sediments on the Baltic sea floor. The aim of this project is to analyse the steps and possible formation processes from the survey data. The data used are taken from the acoustic instruments multibeam echosunder and Chirp sonar sediment profiler. The multibeam reveal the seafloor topography and can detect water column features. The Chirp sonar produce sub-bottom profiles showing the sediments down to some tens of meters underneath the sea floor. The multibeam data show multiple crescent shaped steps as well as elliptically shaped “pockmarks”. Water column data show what could be interpreted as seeps from the sea floor under these features. The sub bottom profile show deformation and fluid signatures under the steps. Gas signatures and what could be other fluids are present. The interpretation concludes that the formation could be from either gas or groundwater seeps. No definitive conclusions can be made from the data available for the present study, and apetrophysical or geochemical study of the study area cold provide further understanding of the formation of the steps.


**Keywords:** Multibeam, Sub-bottom Profiler, Stockholm Archipelago, Geomorphology, Baltic Sea, Gas Seeps, Methane Gas, Fluid Migration, Groundwater, Acoustic Units, Sediment Profile

## Table of Content

# 1. Introduction

## 1.1 Mapping Submarine Glacial Landforms

Mapping of the sea floor can help reveal the traces left behind from the latest glacial retreat. Marine geologists use acoustic methods such as the multibeam and sub-bottom profiler for surveying the sea floor. These methods can yield high resolution images of the sea floor and the sediments below the sea floor. Because of their ability to image both the surface forms and sediments at depth, acoustic methods are suitable for studying the landforms and sediments in marine environments in areas affected by glaciations, such as coastal areas of Sweden.

## 1.2 Study Area

The study area is located close to the island of Askö in the south part of the Stockholm Archipelago in the Baltic Sea. As seen in the nautical map from the Swedish Maritime Administration (figure 1) the maximum depth in the area is 43 m and the water is brackish with a salinity of around 7‰ (Östersjöcentrum, 2017).

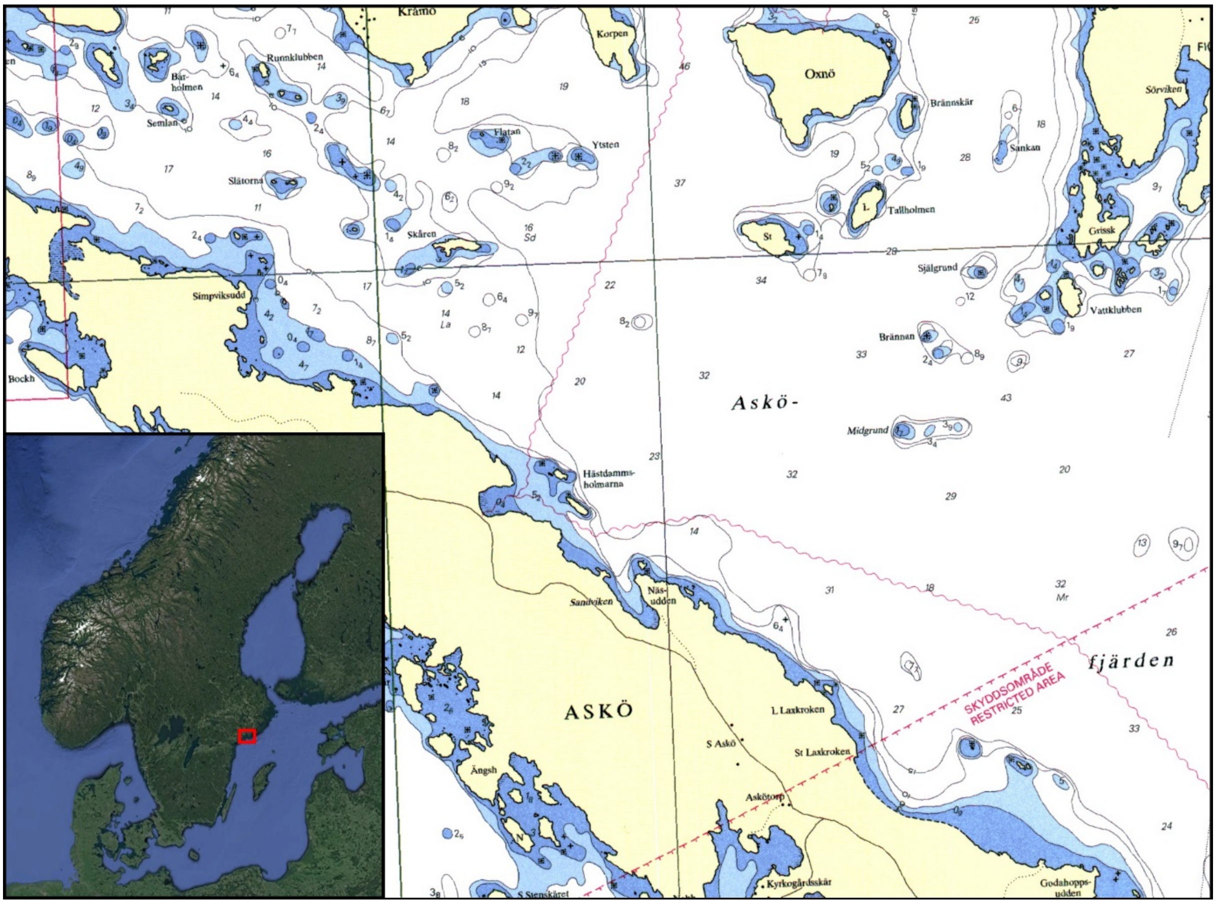


Figure (1). The study area is shown in relation to the rest of Sweden and shows the study area in the southern Stockholm archipelago and north east of the island Askö. The figure combines google earth images and nautical map from the Swedish Maritime Administration.

The fresh water supply comes upstream from lake Mälaren flowing through Himmerfjärden and out into the Archipelago to the study area. Himmerfjärden consists of 79% transport/erosional bottoms meaning that more sediments are carried out into the archipelago than deposited (Jonsson, et al., 2003). The estimated sediment accumulation for water bodies such as Asköfjärden is about 1000 $g/m^2$ per year (Jonsson, et al., 2003). Asköfjärden and the nearby Fifångdjupet are classified by Jonsson, et al. (2003) as areas where the water exchange is relatively large due to the close exposure to the open sea. This implies that the area contains erosional bottoms rather that depositional bottoms. Erosional bottoms can occur down to a depth of 70 m and is driven by underwater currents which are present in the area (Jonsson, et al., 2003). Ocean currents are driven by wind (Nichols, 2009) and wind can also generate waves in the Baltic Sea with wave bases as deep as 80 m in some places (Jonsson, et al., 2003). According to the ice maps of the Swedish Meteorological and Hydrological Institute (SMHI), the area is ice covered during the winter months which could slow down bottom erosion processes in the area however.

Previous marine geophysical surveys in the Askö study area by Jakobsson et al. (2016) reveal landforms resembling terraces on the sea floor which resemble underwater features mentioned by Söderberg & Flodén (1997) in other areas of the archipelago. These features were interpreted by Söderberg & Flodén (1997) and Jakobsson et al. (2016) as being formed by ground water sapping through the clay layers, undermining the overlying sediments and eventually causing collapse. Jakobsson et al. (2016) also show in sediment profiles how deformed layers in the sediments display rising fluid, creating a lens like feature. How fluid escape causes crater like features on the sea floor can be explained by pressure build-up under the sediments due to a low permeability seal (O'Regan, et al., 2015). When the pressure becomes too high the fluids travel upwards through the sediments lowering the porosity. After fluid escape the sediments become remoulded and can leave behind a crater like feature (O'Regan, et al., 2015). This phenomenon is not limited to the Baltic Sea, as it has been encountered on shelf areas worldwide (Post, et al., 2003). A study of submarine valley formation off the coast of New Jersey has proposed ground water flow as an explanation for these features (Robb, 1984). Gas seeps also has the potential for changing the sea floor morphology and as noted by Söderberg & Flodén (1997), this is a common occurrence in the archipelago. Söderberg & Flodén (1992) investigates the presence of methane gas along tectonic lineaments in the archipelago. The landform "pockmark", a crater like the feature discussed in O'Regan, et al. (2015) found in the archipelago was interpreted to be created by degassing in the sediments. Gas signatures in geophysical sediment profilers can be seen as a sudden blurring of data called gas blanking (Jones, et al., 2010). Blanking is generated from the absorption of the acoustic wave by the gas leaving a high amplitude signal in the sediment profile (Davis, 1992). Gas can also cause acoustic turbidity which are bubbles of gas in the sediments leaving a black smear in the sediment profile. The bubbles disperse the incoming signal so no information can be gathered underneath the gas (Davis, 1992 & Judd & Hovland, 1992).

### 1.3 Project Goals

The goal of this project is to analyse and interpret the geomorphological features on the sea floor north of Askö in relation to fluid flow, glacial history and paleoceanography using acoustic data acquired with marine geophysical mapping methods.

### 1.4 Geological Background

The bedrock in the Stockholm Archipelago mainly consists of Precambrian crystalline basement rocks, mostly granites and gneisses (SGU bedrock map and Winterhalter et al., 1981) as part of the Fennoscandian shield which cover Sweden, Norway, Finland and western parts of Russia (Lundqvist, et al., 2011). The bedrock was created during the Svecofennian orogeny ranging from 1950 Ma to 1750 Ma which was a time of intense volcanism and build-up

of continental crust (Lundqvist, et al., 2011). The most common types of sediment in the study area is glacial, and were deposited as the ice sheet retreated. Sediments deposited in more recent time consisting of clay and silt are called postglacial sediments (Andrén et al., 2011). According to the SGU 1:100 000 marine geological map the sea floor sediments are mainly glacial clay but also glacial silt/fine sand with recent sediments deposited on top. Closer to the islands in the area we can find postglacial sand, fine sand and gravel.
Towards the end of the Weichselian glaciation, the southern parts of Sweden became ice free around 15500 BP. This marks the start for isostatic rebound for the Svecofennian continental crust (Lundqvist, 2004) which was rising faster than the ponding of the meltwater which lead to the forming of the Baltic Ice Lake (Andrén et al., 2011). At 11550 BP, the Baltic Ice Lake, a fresh water lake draining through narrow passage in Öresund and at Mt. Billingen when the ponding exceeded isostatic rebound. Varved sediments (clayey-silt and non-organic) was deposited in the Baltic from the retreating ice and the rebound was high during this stage (Björck, 2008). An ice advance during the cooling during the Younger Dryas starting at around 12800 BP closed the Mt. Billingen drainage, damming the ice lake even more (Andrén et al., 2011). This caused more water to be drained through Öresund, which also experienced rebound. When the climate warmed at the end of the Younger Dryas at about 11600 BP the ice margin retreated, causing a sudden drainage of the Baltic Ice Lake at Mt. Billingen (Björck, 2008). The result of the drainage was a lowering of the Baltic Ice Lake surface of ca 25 meter in 1-2 years (Jakobsson et al., 2007). The drainage of the Baltic Ice Lake marks the next sea stage in the development of the Baltic Sea (Andrén et al., 2011).

During the Yoldia Sea stage (11700-10700 BP) the ice retreated faster due to warming during the beginning of the Holocene (Andrén et al., 2011) and connected the Baltic Ice Lake to the Kattegat (Lundqvist, et al., 2011) through straits across south central Sweden. During the Yoldia stage the Baltic Sea water is at sea level and this marks the first time these waters became brackish, during a short time interval which ended due to ongoing isostatic rebound. More rebound caused the Yoldia Sea to become closed off again creating the Ancylus Lake around 10500 BP and when the ice had disappeared the land was still rising. During the Littorina stage around 8000 BP the sea reached its saline highpoint due to deeper and wider inlets in Öresund and lowered fresh water supply (Andrén et al., 2011) probably due to damming in the Ancylus stage causing submerging of previously uplifted areas. The salinity increase can be seen in the sedimentary record as increase in organic content from a more diverse and living sea (Björck, 2008). The Littorina stage continues to the present.

# 2. Methods

## 2.1 Geophysical Methods

High-resolution sub-bottom profilers such as the chirp sonar used for this study generate a sound wave by passing electricity through a piezo-electric material. This causes the piezo-electric material to expand and contract and doing so transmits sound. The transmitted sound wave is later echoed back from the sea floor or internal reflectors in the below sea floor to the receiver and the two-way travel time (TWT) is recorded. This can be converted to depth using equation (1):

$$d = v * \frac{TWT}{2} \tag{1}$$

where v is the sound wave velocity (Jakobsson et al., 2016). Acoustic waves obey the same natural laws as light passing through different media and therefore we can describe the behaviour of sound waves using Snell's Law shown in equation (2):

$$\frac{\sin \theta_1}{v_1} = \frac{\sin \theta_2}{v_2} \tag{2}$$

where $\theta_1$ is the incidence angle, $v_1$ is the velocity of the incidence wave, $\theta_2$ is the refraction angle and $v_2$ is the refracted wave velocity (Jakobsson et al., 2016). The wave reflection coefficient ($\mu_0$) is a measure of the strength of the reflected acoustic wave, and is dependent on the acoustic impedance contrast of the lithological layers as is described in equation (3):

$$\mu_0 = \frac{I_2 - I_1}{I_2 + I_1} = \frac{v_2 * \rho_2 - v_1 * \rho_1}{v_2 * \rho_2 + v_1 * \rho_1} \tag{3}$$

where $I_1$ is the acoustic impedance of the first lithological layer, $I_2$ is the acoustic impedance of the second layer, $v_1$ is the acoustic wave velocity in the first layer, $v_2$ is the velocity in the second layer, $\rho_1$ and $\rho_2$ is the bulk density in the first and second layer the beam passes through (Mosher & Simpkin, 1999), see figure (2).

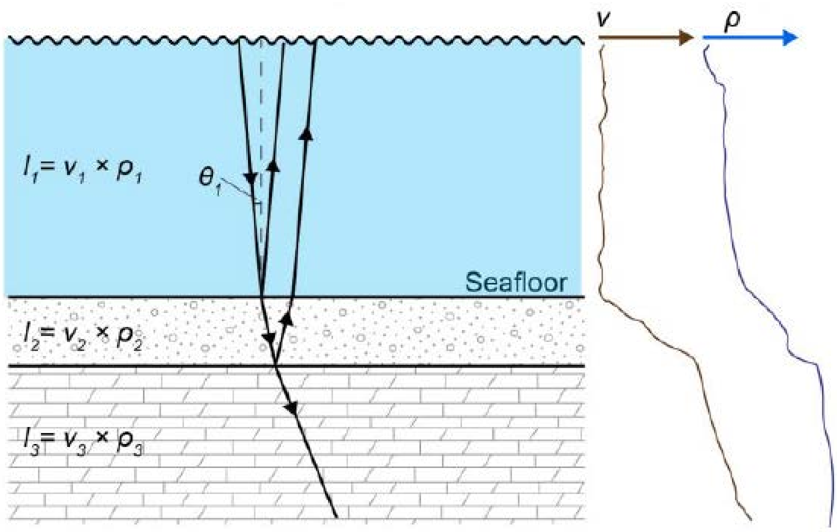


Figure 2. Image from Jakobsson et al. (2016) showing the principle behind SBPs where the incoming signal is both reflected from the sea floor and refracted down the sediments. The refracted beam can also be reflected and refracted as a new sediment layer of different acoustic impedance. The profiles to the right shows the sound velocity and density difference in the changing media.

The area covered by the sound beam is determined by the footprint ($D_f$), which is calculated using equation (4):

$$D_f = 2 * H * \tan\left(\frac{\alpha}{2}\right) \qquad (4)$$

where H is the distance from sound source to the sea floor and α is the beam angle (Jakobsson et al., 2016). The beam angle is the angle the beam has when leaving the transducer source and is dependent of the interference pattern generated by the apparatus and is determined by the frequency of the sound wave and the length of the transducer (Jakobsson et al., 2016). The beam angle can be calculated using equation (5) below (Jakobsson et al., 2016):

$$\alpha = \frac{60 * \lambda}{\emptyset} \qquad (5)$$

from the wavelength of the sound wave (λ) and the transducer length (Ø).

The resolution of the data is the minimum distance that two different objects must be separated to be distinguished in the sonar reading as individual objects vertically or horizontally. Resolution in all signal processing is determined by the Nyquist Theorem which states that the minimum sampling density must be twice the frequency of the signal. If the sampling density is lower than this we will experience aliasing, which is a form of signal distortion (Jakobsson et al., 2016). In vertical resolution consideration must be taken to water depth meaning that for shallower waters with depth less than 100 m the frequency should be higher than 200 kHz with a wavelength shorter than 0.75 cm and for larger depths of more than 1.5 km the frequency should be between 12 kHz and 50 kHz with a wavelength between 12.5 cm and 3 cm (Jakobsson et al., 2016). This is because the energy of a high frequency signal is more easily absorbed in the sea water. With a long wavelength (i.e. low frequency), the beams can reach longer but the resolution will be lower (Jakobsson et al., 2016). The ability to distinguish the difference between two objects vertically acoustic data is determined by the Rayleigh criterion which states that two objects must be separated a quarter of the wavelength as stated by equation (6):

$$R_v = \lambda * \frac{1}{4} \qquad (6)$$

where $R_v$ is vertical resolution and λ is the wavelength (Jakobsson et al., 2016). The ability to resolve objects horizontally on the sea floor is also determined by the 1$^{st}$ Fresnel zone since everything outside this zone will alternate between constructive and destructive interference. The 1$^{st}$ Fresnel zone radius is determined with equation (7):

$$R_F \approx \sqrt{\frac{H * \lambda}{2}} \qquad (7)$$

Where $R_F$ is the Fresnel zone radius, H is the water depth and λ is the wavelength (Jakobsson et al., 2016). For the multibeam sonar system used here, the horizontal resolution is for a signal of 300 kHz and a water depth at ~40m gives a resolution of 31.6 cm whereas the chirp sonar has a vertical resolution determined by equation (8);

$$Rv_{chirp} = \frac{v}{(2 \times B)} \qquad (8)$$

where v is the sound speed velocity in sea water (approximated to 1500 m/s), B is the bandwidth ranging from 2 kHz to 16 kHz which is 14 kHz, giving a vertical resolution of about 5 cm.

### 2.1.1 The Sub-Bottom Profiler

The previous methods mentioned were for measuring the sea floor topography; sub-bottom profilers (SBP) however are powerful tools of looking down through the sediment layers. The SBP used is an EdgeTech SB-216S Chirp Sonar. The chirp sonar transmits an FM signal sweeps a range of frequencies spanning from 2 kHz to 16 kHz which enables the chirp to generate a sound pulse stronger than ordinary SBPs (Jakobsson et al., 2016). The behaviour of the transmitted signal obeys the physical laws described in equations (2) and (3) implying that the beams will either reflect of refract when encountering a geological layer of different acoustic impedance. The reflection coefficient in equation (3) is determined by the impedance and sound velocity in the layer which manifests in the produced SBP image (Lurton, 2010). The chirp sonar also makes use of a so called matched filter (figure 3) that matches a compressed transmitted FM signal to the received signal which allows a collapse of the signal leaving an amplified signal to generate higher penetration and resolution (Schock et al., 1989).

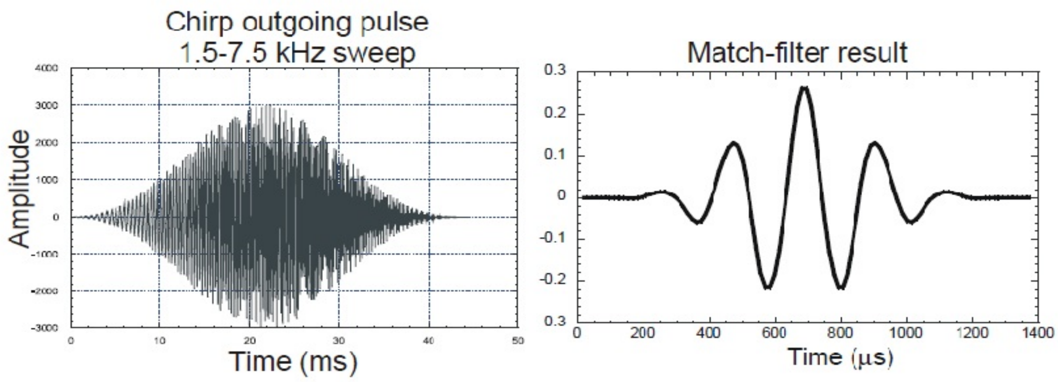


Figure (3). Showing the matched filter cleaning the outgoing Chirp pulse when returned to the receiver, figure from Mosher & Simpkin, (1999). Notice the shorter wavelength and lower amplitude.

### 2.1.2 The Multibeam Echosounder

The multibeam echosunder used is a KM EM2040 with available frequencies of 200, 300 and 400 kHz and a footprint of 1°x1°. The multibeam echosounder system is several transducers that is mounted along the ship, transmitting a fan shaped beam or a swath beam sweeping the sea floor. The receiver hydrophones are rotated 90° to the transmitted beams in a Mills Cross configuration, i.e. mounted across the ship, covering square footprints over the transmitted area, see figure (4). This generates data of a detailed sea floor topography image (Jones, 1999 & Jakobsson et al., 2016).

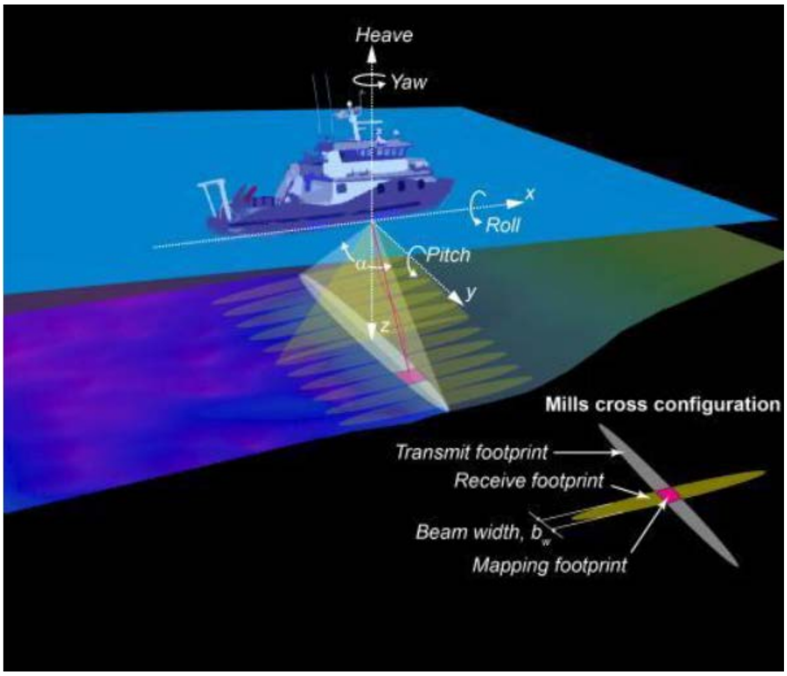


Figure 4. The MBES with the Mills Cross configuration from Jakobsson et al. (2016) where the beam angle (α) is determining the swath of transmitted footprint as well as the multiple beams indicated with yellow colour in the footprint.

For a multibeam survey a sound velocity profile (SVP) must be constructed to calculate the different velocities in the water column for accurate imaging. This can be determined either with measuring the sound speed directly or with using a conductivity, temperature and depth (CTD) probe and using the data with the Mackenzie Equation, seen in equation (8), at each CTD measure (Jakobsson et al., 2016):

$$v = 1448.96 + 4.591 * T - (5.304 * 10^{-2}) * T^2 + (2.374 * 10^{-4}) * T^3 + 1.340 * (S - 35) + (1.630 * 10^{-2}) * D + (1.675 + 10^{-7}) D^2 - (1.025 * 10^{-2}) * T * (S - 35) - (7.139 * 10^{-13}) * T * D^3 \quad (8)$$

where v is the sound speed velocity, S is salinity, T temperature and D is depth. These sound velocities can be calculated with a harmonic mean value for the sound speed which accounts for the time that the sound pulse will spend in the different layers in the water column (Jakobsson et al., 2016). Further corrections during acquisition are made for the vessel's heave, pitch, roll and yaw during acquisition since it can change the geometry of transmitted and received beams (Jakobsson et al., 2016).

## 2.2 Data Acquisition and Processing

The multibeam data was gathered during September 2nd to the 3rd 2012 and August 31st to the 1st of September 2013 with research vessel (RV) Skidbladner which is an Arronet 20-5 cs (5,6x2,4m) aluminium boat with a weight around 2 ton fully equipped. The multibeam is a Kongsberg EM2040 (200-400 kHz 1°x1°) mounted on the bow of Skidbladner.

Multibeam data was imported into QPS Qimera for processing. The data was compiled into a 3D environment mirroring the survey from the study area using the same spatial information for displaying the data set. In Qimera superfluous data that was not part of the survey area was deleted. The data was using a SVP built from data gathered on the day of the survey. Once the data was displayed as a surface as seen in figure (5a) the data was imported to QPS Fledermaus for analysis. The multibeam data used for investigating the water column was imported into FMMidwater for analysis. First the datafiles must be converted to general water column (GWC) file from the "wcd" files while using the original "all" files for its navigational reference information. If a feature in the water column profile is found using FMMidwater the chosen profile can be imported into Fledermaus for further analysis as a scene file.

The goal is then to import the water column data into Fledermaus for analysis. The FMMidwater can use a fan view or a beam view for manual search through the water column, see figure (5a-b). There is an option to manually go through all the profiles and single out every feature manually but to save time, the feature detection tool was used instead. The feature detection tool in FMMidwater was used on the chosen multibeam track and the tool extracts features not interpreted as water by the algorithm.

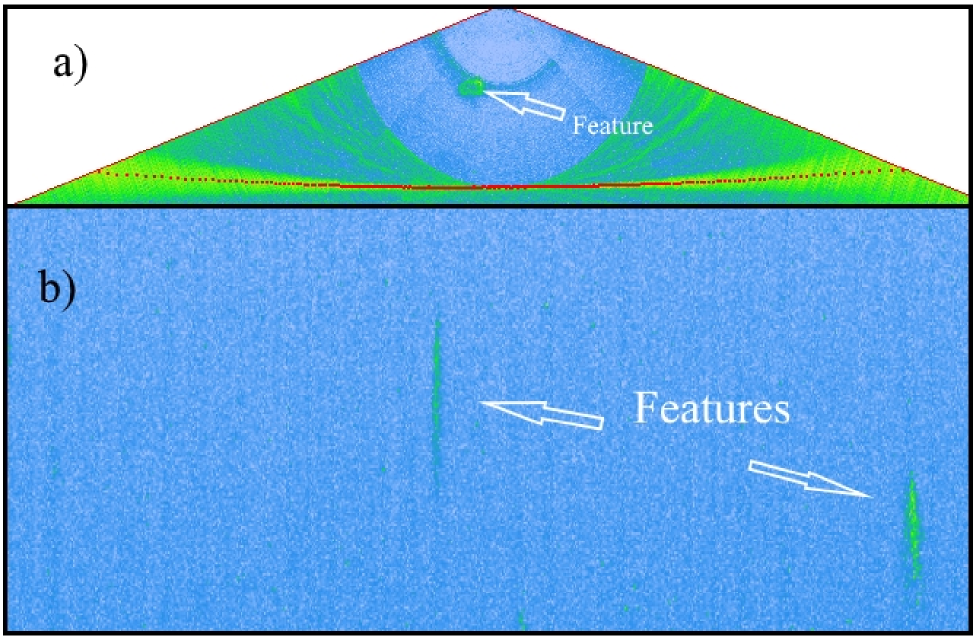


Figure (5) to illustrate how features can be found in FMMidwater in fan view a) and beam view b). The feature detection tool will extract features (green/yellow) not interpreted as water (blue).

Sub-bottom profile data was collected with RV Aurelia on the 9th of April 2013. The RV Aurelia is a 17 m long with a weight of 44 ton and can reach a max speed of 9.5 knots. Analysing sub-bottom profile images was done in the open source software OpendTect V6.0.1 at Stockholm University. The original survey SEG-Y files were processed beforehand

and ready for analysis. OpendTect allows the SBPs to be shown in a 3D environment mirroring the study site as seen in figure (6).

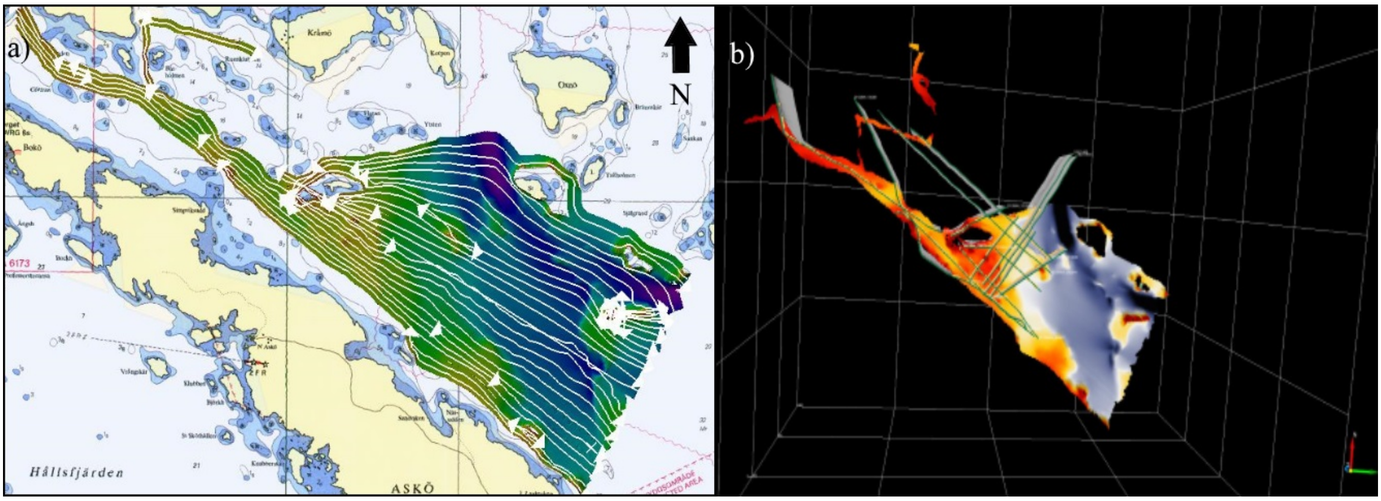


Figure (6). Left a) shows the processed multibeam data in QPS fledermaus. The yellow lines show the RV surveying tracks and the difference in colour along the tracks marks depth differences. Also projected is the nautical map for reference. Right b) OpendTect workspace with the green lines representing the SPBs and projected is a 3D environment of the study area.

## 3. Results

The results are from two interesting sections in the study area with visible step like features in the SBP data analysed in OpendTect. These two areas can be seen on the multibeam map of the study area in figure (7). There is a similarity between the two areas which is that they both lie in a slope where water depth goes from about 14 m to 16,5 m. The SPB data is used as a foundation in which multibeam water column data was analysed in FMMidwater and combined with the multibeam data in Fledermaus.

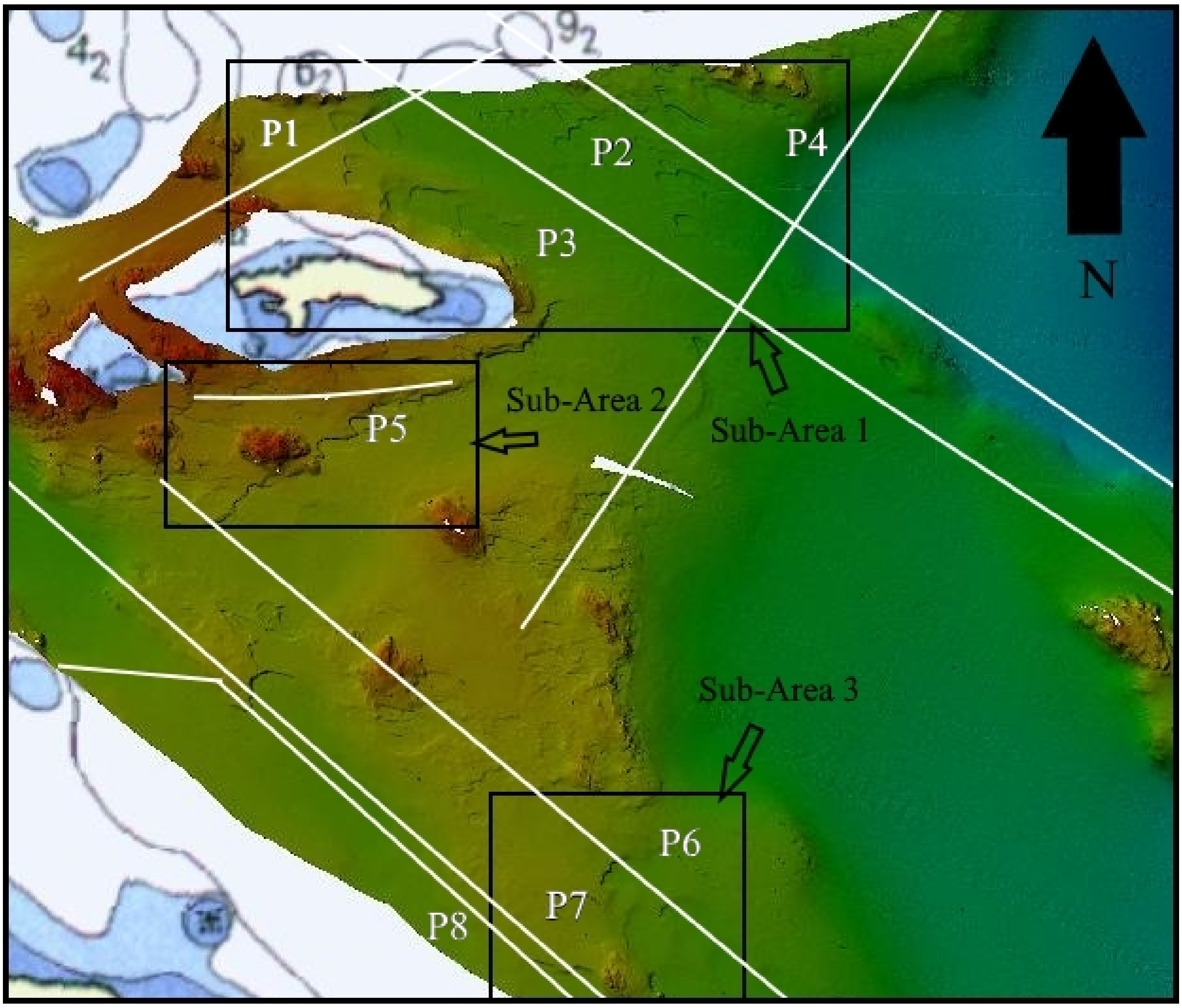


Figure (7). The white boxes represent sub-area 1, sub-area 2 and sub-area 3 respectively. The sub-areas were chosen based on step signatures in the SBP profiles. The track lines are in white and the SBPs in the area are also marked with a P for profile and numbered as they appear in the results section.

## 3.1 Sub bottom profiling

### 3.1.1 Sub-Area 1

SBP data in sub-area 1 was of good quality and 4 profiles were chosen for the project in sub-area 1. The SBPs in sub-area 1 reveal 6 different lithological units described in table (1). The SBPs can be seen in their original state in appendix (III). The profile in figure (11) is used as a cross cut between profiles in figure (9) and (10). Going from south-west to the north-east. Whereas the other profiles go from north-west to south-east.

| Acoustic Units Sub-Area 1 | | |
|---|---|---|
| Unit | SBP Example | Description |
| I | 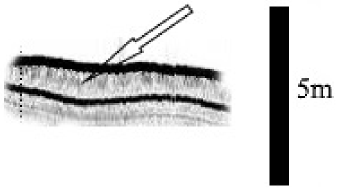  | Strong reflector at sea floor but no internal reflectors visible in this 1 m thick layer. |
| II | 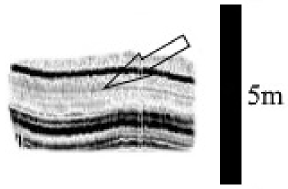  | Low intensity reflectors alternations between stronger and weaker is visible. The layers vary in thickness from 1 m to around 1,5 m. |
| III | 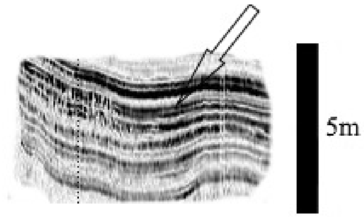  | Varying intensity in reflectors varying from strong and weak in reflection. This unit is around 4 m thick. |
| IV | 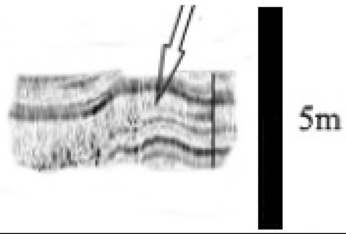  | A 1 m layer with more closely packed weak reflectors layering. |
| V | 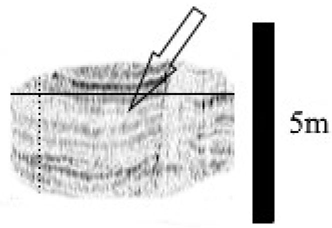  | 3 m of weak reflectors making it hard to distinguish the alternations. |
| VI | 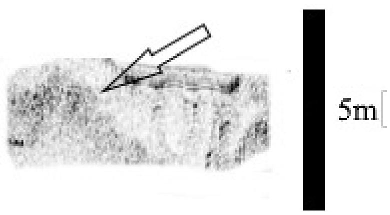  | No further transmitting of beam beyond this point marking an acoustic basement. |

Table (1). Interpretation of acoustic units in sub-area 1 for SBP data.

As seen in the following figures there are many signs of fluids in the sediments. Steps are present in all the profiles because of the scope of the project focuses on those features. Artefacts are present in the form of multiples which are multiple echoes of the strongest reflector which has been reflected one or more additional times between the water surface and the seafloor before being detected (Jakobsson, et al., 2016), as seen in figure (8). In figure (8),

(9) and (11) a bowl like feature fan be seen, resembling two steps facing each other. In figure (8) and (9) a small outcrop of the acoustic basement material can be seen.

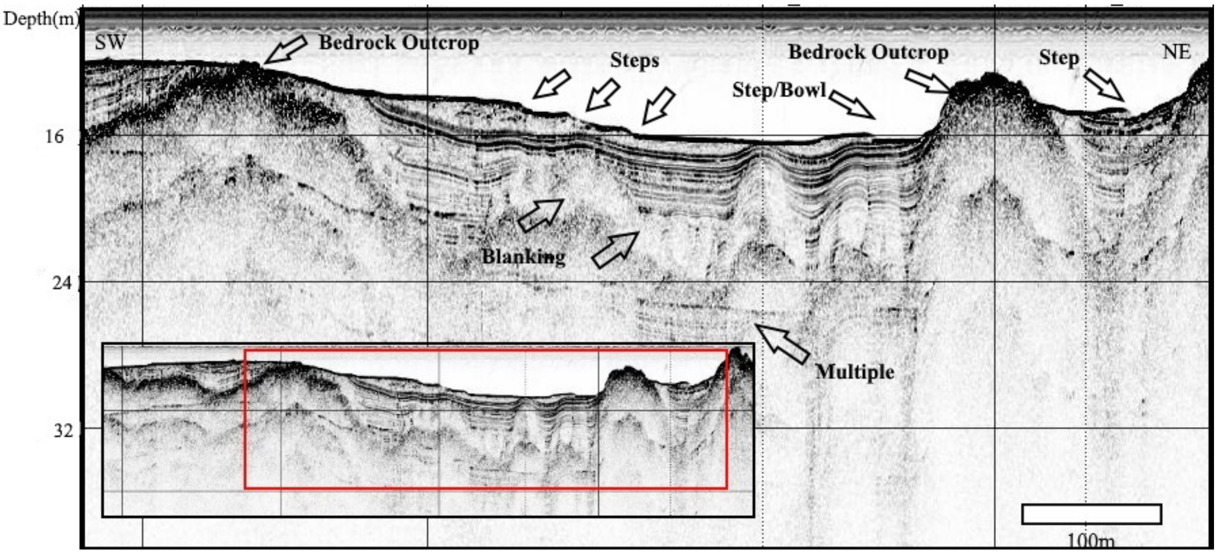


Figure (8). Profile 20130904_125107 (P1). Here several deformation columns in the sediment layer underneath step and bowl like features are present. Also, small outcrops of bedrock can be seen.

The steps are found in acoustic units I to II and halts at III. Steps vary in sharpness from a slope of about 90° and as slant as about 45° in some places. As seen in the profiles some steps face each other forming a bowl like feature in which the steps do not seem to be the same height. Convex deformation looking like lenses bulging upwards through the columns and are present in all the profiles. Deformed sediment layers seem to follow the bottom topography. In figure (8) the acoustic basement reflector shape is reflected by the layers above forming a drape. Also in figure (8) however there are blanked sediments and deformed layers above.

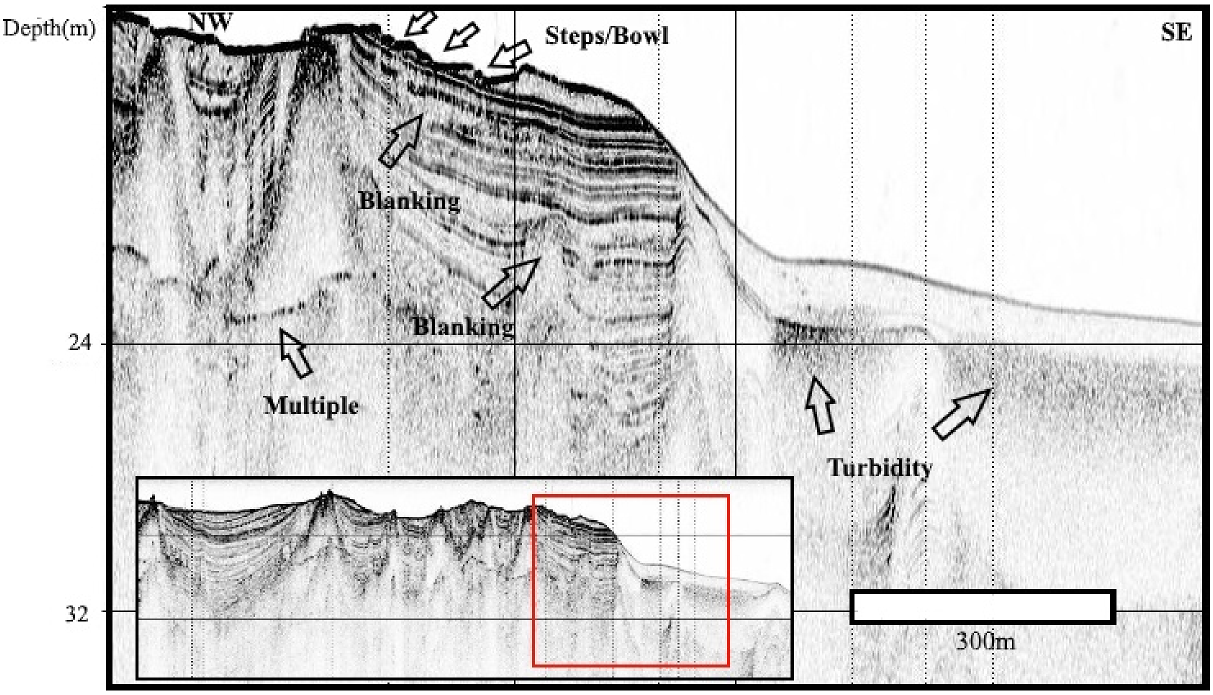


Figure (9). Profile 20130904_114640 (P2) shows steps along with two steps facing each other forming a bowl like feature along acoustic unit III. Acoustic turbidity in sediments can be seen in the deep parts to the south-east as well as in the sediments at shallower depths. A bulging feature appears to be blanking out the sediments.

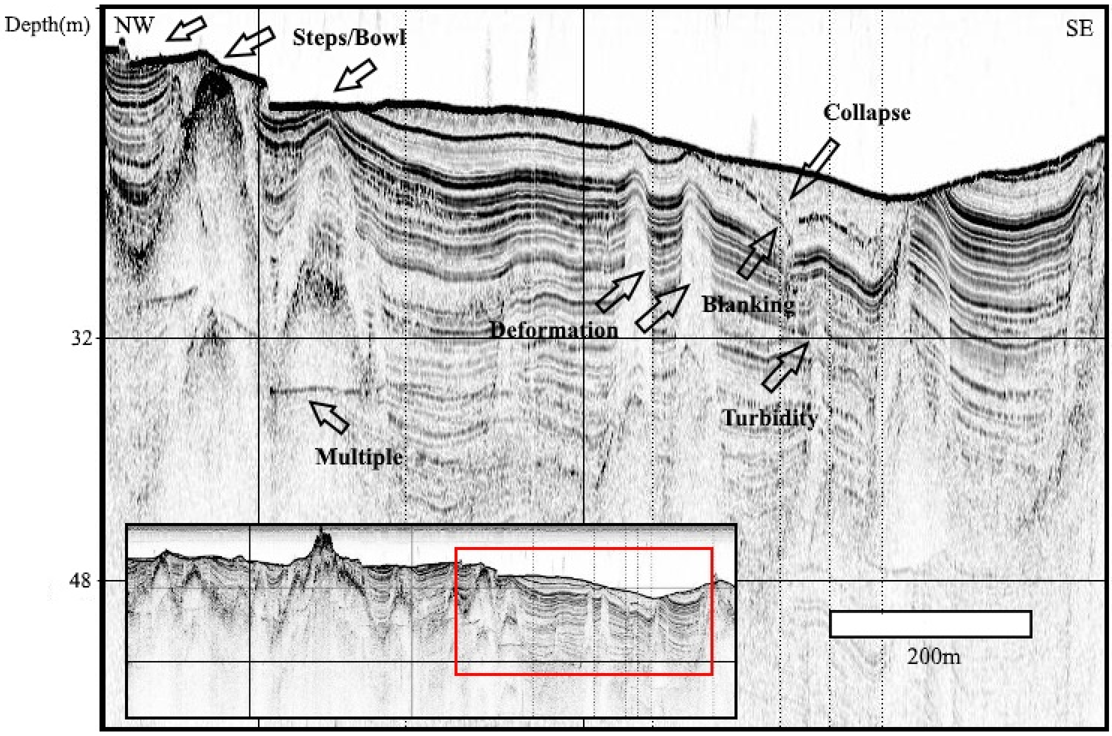


Figure (10). Profile 20130904_092941 (P3) shows distinct steps with possible turbidity underneath. The tallest step faces a step of shorter height and a steeper slope which could be a bowl feature. A part of the sediments seems to de slumped downwards and accompanied by blanking and turbidity to the south-east.

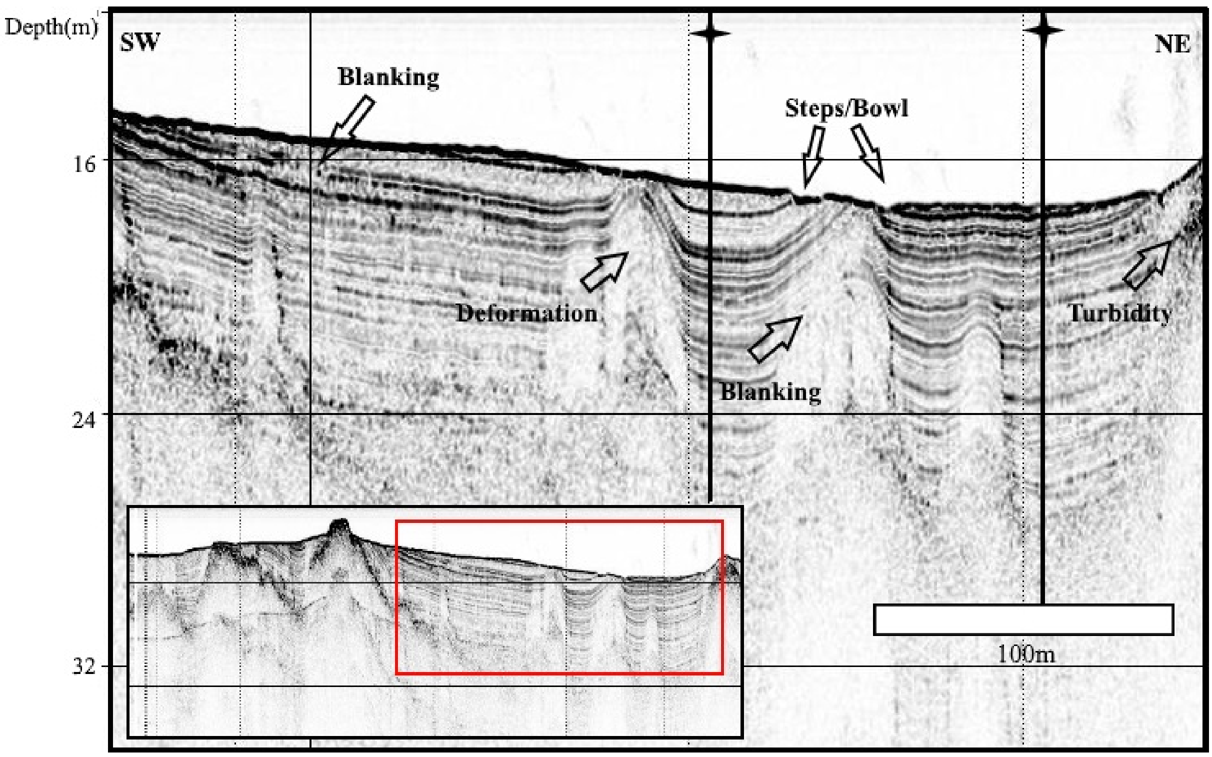


Figure (11). Profile 18311424 (P4) which is a profile that intersects the other profiles the thick line with a cross to the SW denotes where the profile in figure (9) intersects and the line to the north-east donates where figure (10) intersects.

### 3.1.2 Sub-Area 2

One SBP in the area was taken and it is taken at shallower water depths. The profile is blurry which makes features harder to find. The acoustic units found in this area can be seen in table (2) and at least three units can be seen. The first one layer is transparent with no internal reflectors. We also have layers of multiple low to high intensity reflectors as well as other layers with lower intensity reflectors.

| Acoustic Units Sub-area 2 | | |
|---|---|---|
| Unit | SBP Example | Description |
| I | 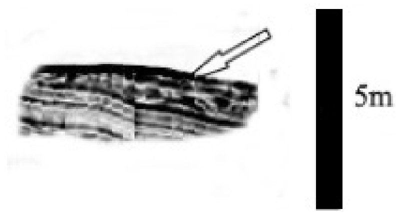  | No internal reflectors visible in this layer. The unit is around 3 m thick in this area. |
| II | 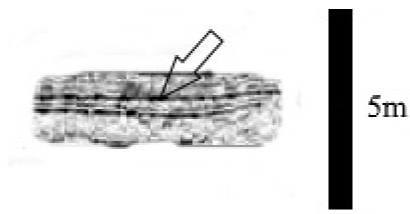  | Varying intensity in reflectors varying from strong and weak in reflection. This unit is around 3 m thick. |
| III | 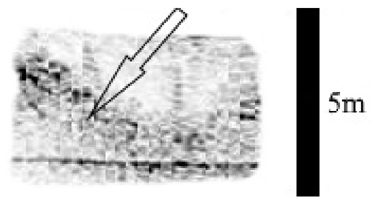  | No further reflectors after this layer. Marking this as an acoustic basement. |

Table (2). The acoustic units present in profile 20130904_090928. The blurry quality of the profiles makes it difficult to see some of the units in the profile.

One step like feature is detected underneath sedimentary layers of intense blanking for 100 m which complicates in which acoustic unit the step belongs in. It is almost impossible to distinguish the reflectors in this stage as the blanking stretches out into deeper waters, see figure (12). A multiple of the sea floor reflector can be seen after the acoustic basement reflector. Also, seen in figure (12) are deformation of sediments forming lens like structures. The lenses are bulging convexly towards the sea floor reflector and some of them are almost entirely blanked out so that no internal reflectors can be seen. One step is visible on the sediment surface below the blanked sediments.

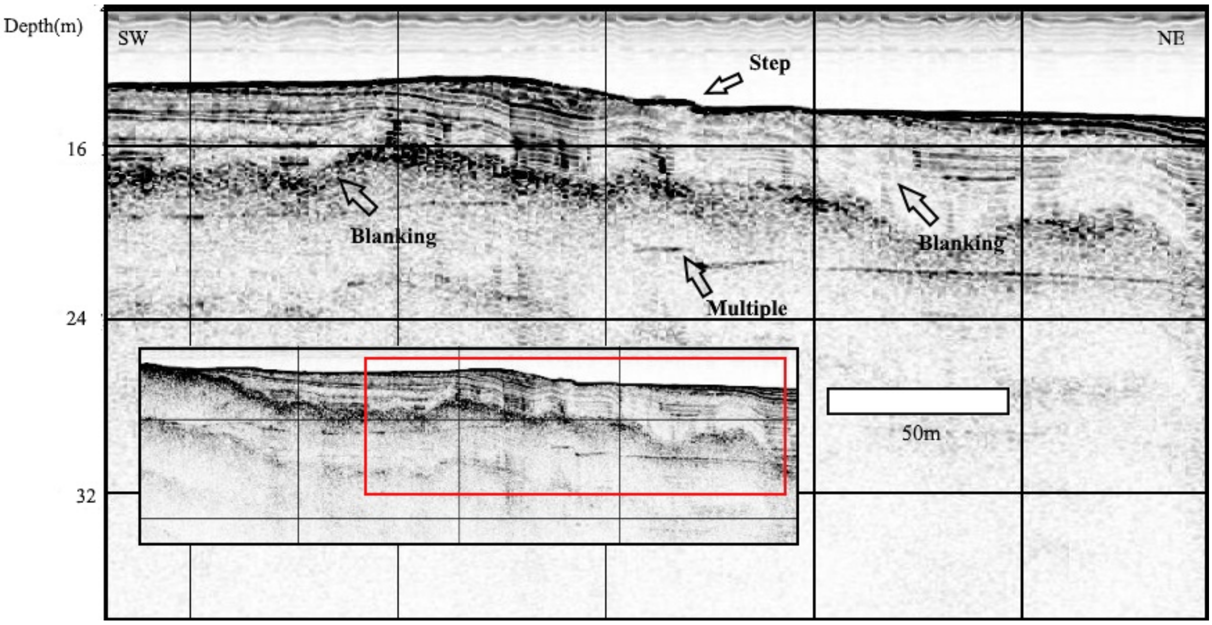


Figure (12). Profile 20130904_090928 (P5) which blanking is seen at the acoustic basement to the south-west. Blanking is also present in the sediment column which is deformed underneath the step feature.

### 3.1.3 Sub-Area 3

The SBP data is of good quality, meaning that acoustic reflections are clearly defined and not noisy and the distinction between water column, sediments and bedrock/till is quite clear. This enables the SBP data to be divided into 7 lithological units from three different profiles. Bedrock can be seen in the form of outcrops and can be traced to the sea floor indicating an acoustic basement. The contact between sediments and the acoustic basement can be a strong or weak reflector making it hard to see it in some cases. In some parts of the profiles there is no internal acoustic reflectors making the unit acoustically transparent. These sediment layers' range in thickness from 0.5 m to 1 m which was calculated from TWT using equation (1). Deeper into the sediments many internal reflectors can be encountered in varying thickness making the sediments appear laminated. In some profiles the reflectors are more prominent generating sharp contrasts and on other parts the reflectors are so weak they can hardly be seen. A collection of the acoustic units is presented in table (3).

| Acoustic Units Sub-area 3 | | |
|---|---|---|
| Unit | SBP Example | Description |
| I | 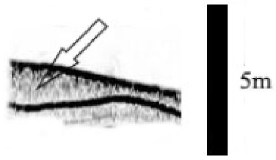  | No internal reflectors visible in this layer. The unit is around 2 m thick in this area. |
| II | 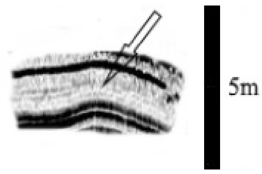  | Low intensity reflectors alternations between stronger and weaker is visible. The layers vary in thickness from 1 m to around 2 m. |
| III | 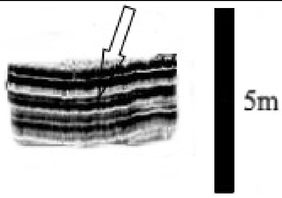  | Varying intensity in reflectors varying from strong and weak in reflection. This unit is around 3 m thick. |
| IV | 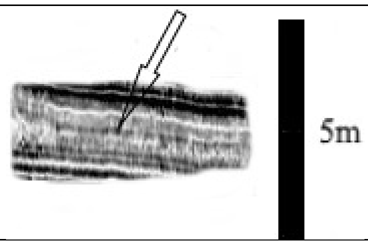  | Weaker in reflection and varies in intensity for around 2 m. |
| V | 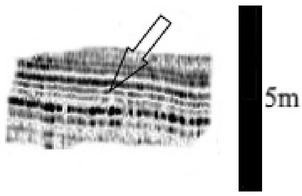  | A layer about 2 m of stronger reflectors alternating from weak to strong. |
| VI | 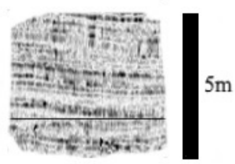  | Weak reflectors in the layer ranging to thicknesses around 6 m to 7 m. |
| VII | 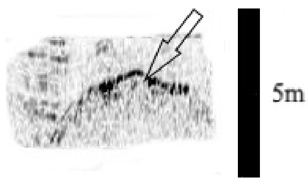  | At this limit the signal cannot be carried further marking this an acoustic basement. |

Table (3). Interpretation of the acoustic units present in sub-area 3.

Multiple step like erosional features can be seen in Asköfjärden as seen in figures (13), (14) and (15). In figure (13) the steps are present in or above acoustic unit III. In figures (14) and (15) it is harder to see because of the blanking. The steps vary in height with the tallest being about 1.5 m. Deformation of the underlying sediments in the form of lenses towards the sea floor can be seen in figure (13). The sediments drape the acoustic basement in some cases however, see figure (14) for example. Additional erosional features can be seen where the continuous strong reflectors appear scraped away which is consistent with erosional bottoms, see figure (13) for example. Blanking is seen in both figure (14) and (15). This blanking is the sudden blurring of otherwise visible reflectors and to the north-west in figure (14).

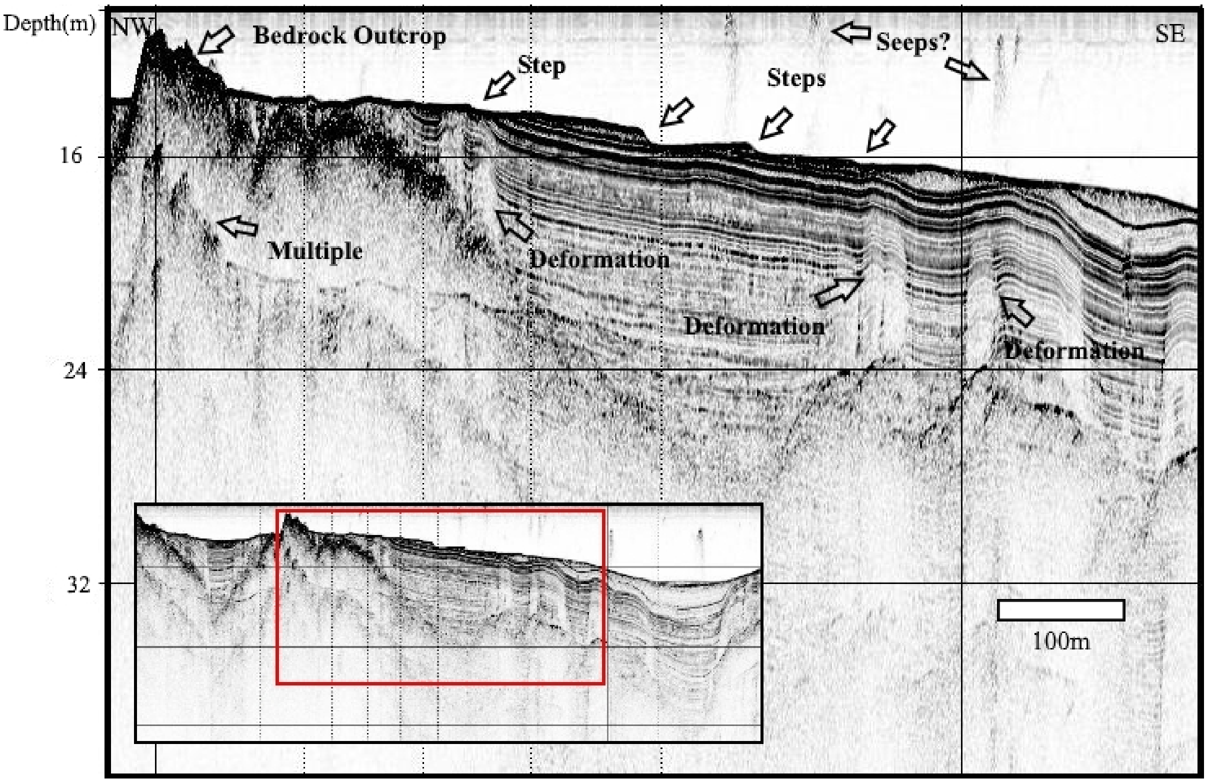


Figure (13). Analysis of profile 20130904_084807 (P6) shows outcropping bedrock as well as deformed layers that has also been seen in Jakobsson, et al. (2016), step like features that has a ~45° slant. The artefact known as multiple is present in the profile as a reflection downward. Acoustic turbidity can be seen in the far south east of the figure.

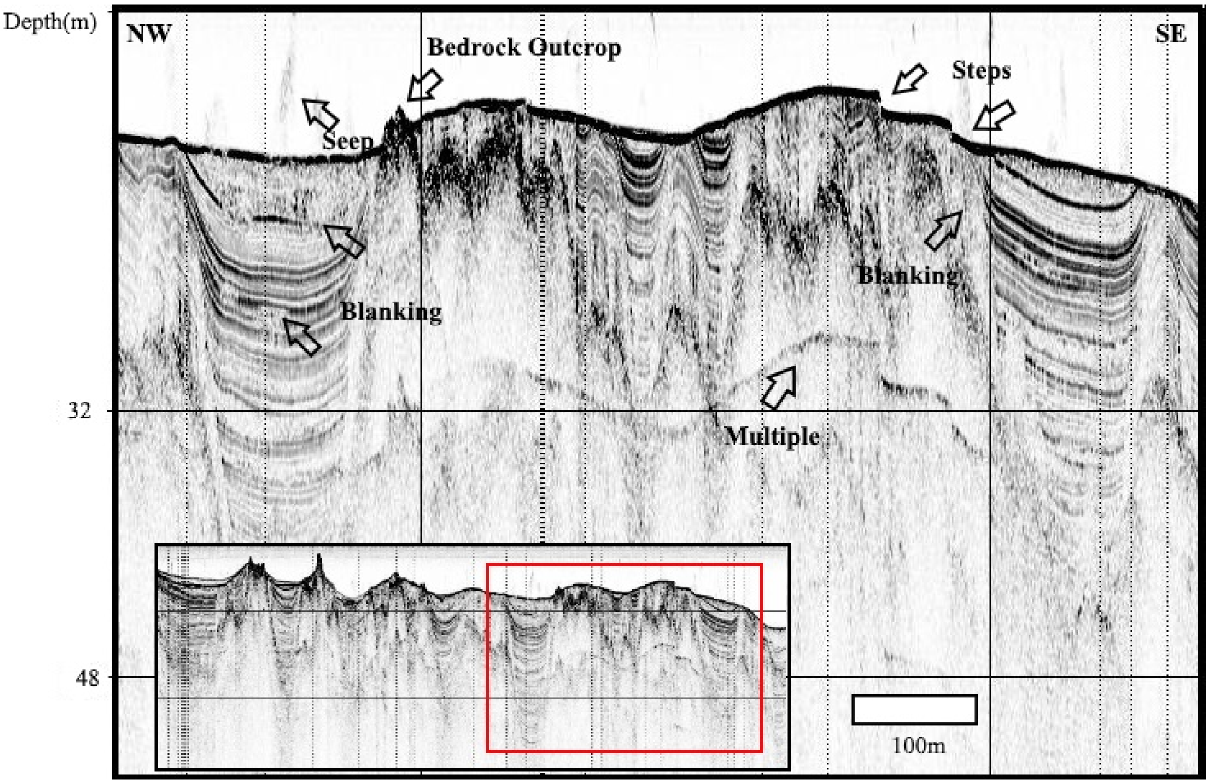


Figure (14). Profile 20130904_105339 (P7) shows distinct steps. Also seen is a multiple coming from the sea floor reflector. Fluid escape into the water column is possibly seen in the layers to the north-west.

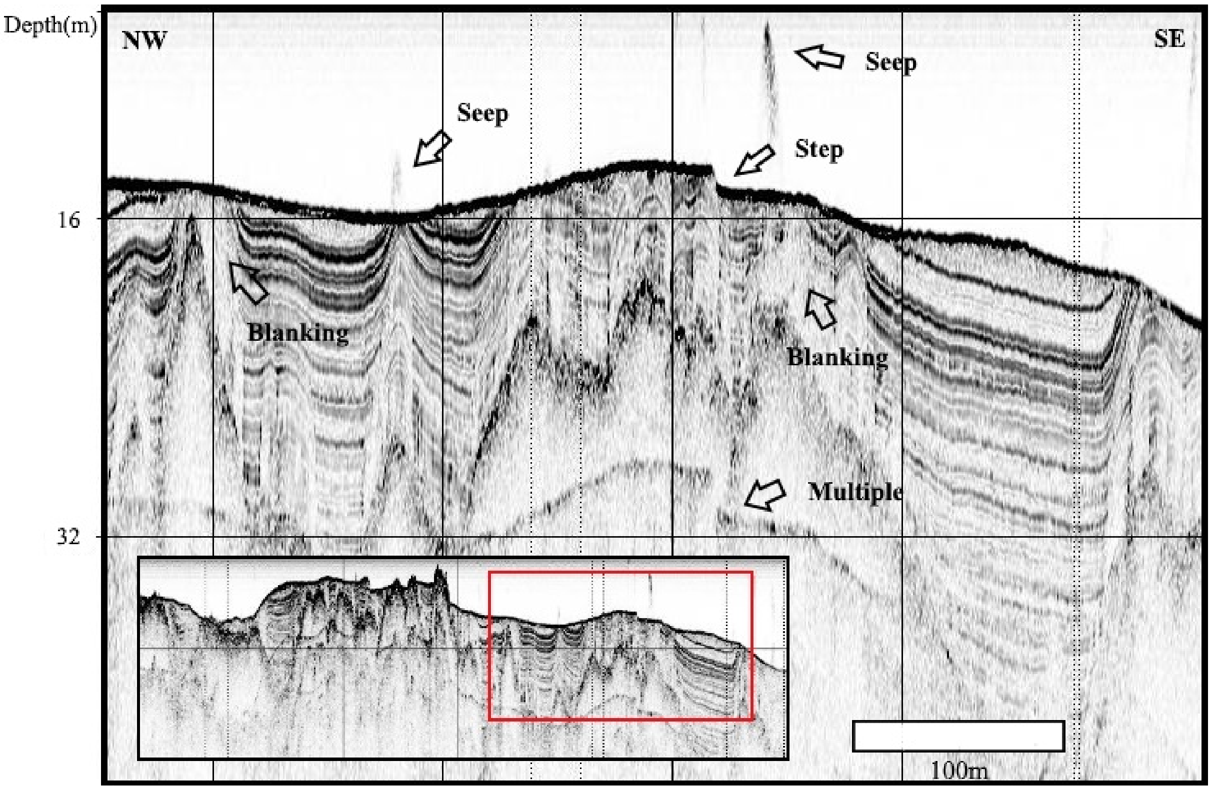


Figure (15). Profile 29051049 (P8) reveals a step feature above sediments with fluid escape and some deformed layers. There is also blanking present in the profile.

## 3.2 Multibeam and Water Column Data

### 3.2.1 Sub-Area 1

Data from the multibeam processing gives a clear image of the seafloor morphology in Asköfjärden. The data shows distinct creasing shaped steps to the west also covered by the SBP data. The steps however are about 1 m in height and has relatively gentle slope of about 45° to about 20° and goes from about 13 m down to 17 m depth, see figure (16). Corresponding three steps can be seen in the SBP data in figure (8) and the line drawn in figure (16a) show the similarity of the profiles.

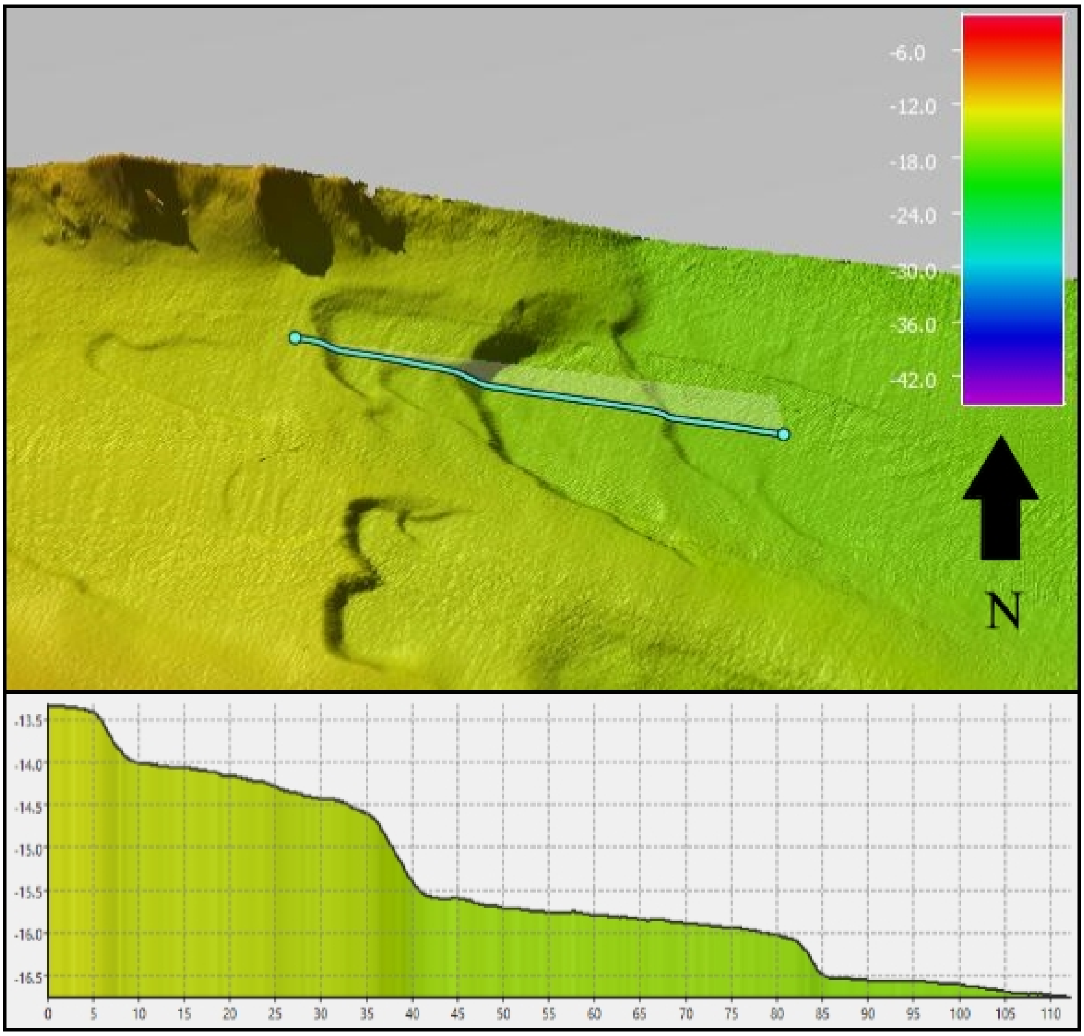


Figure (16). An overhead view in a) showing steps around the island Skåren. A stretch of sea floor 100 m long with three step features at a depth around 13 m to 16,5 m shown in b). These steps can be seen in the SBP figure (8) where we clearly can see the three steps running down.

To the north east are egg (elliptically) shaped features. These features are clustered together at roughly 18 m depth. They are about 10 m along the short axis and about 60 m along the long axis and the largest one is about 1 m deep, see figure (17).

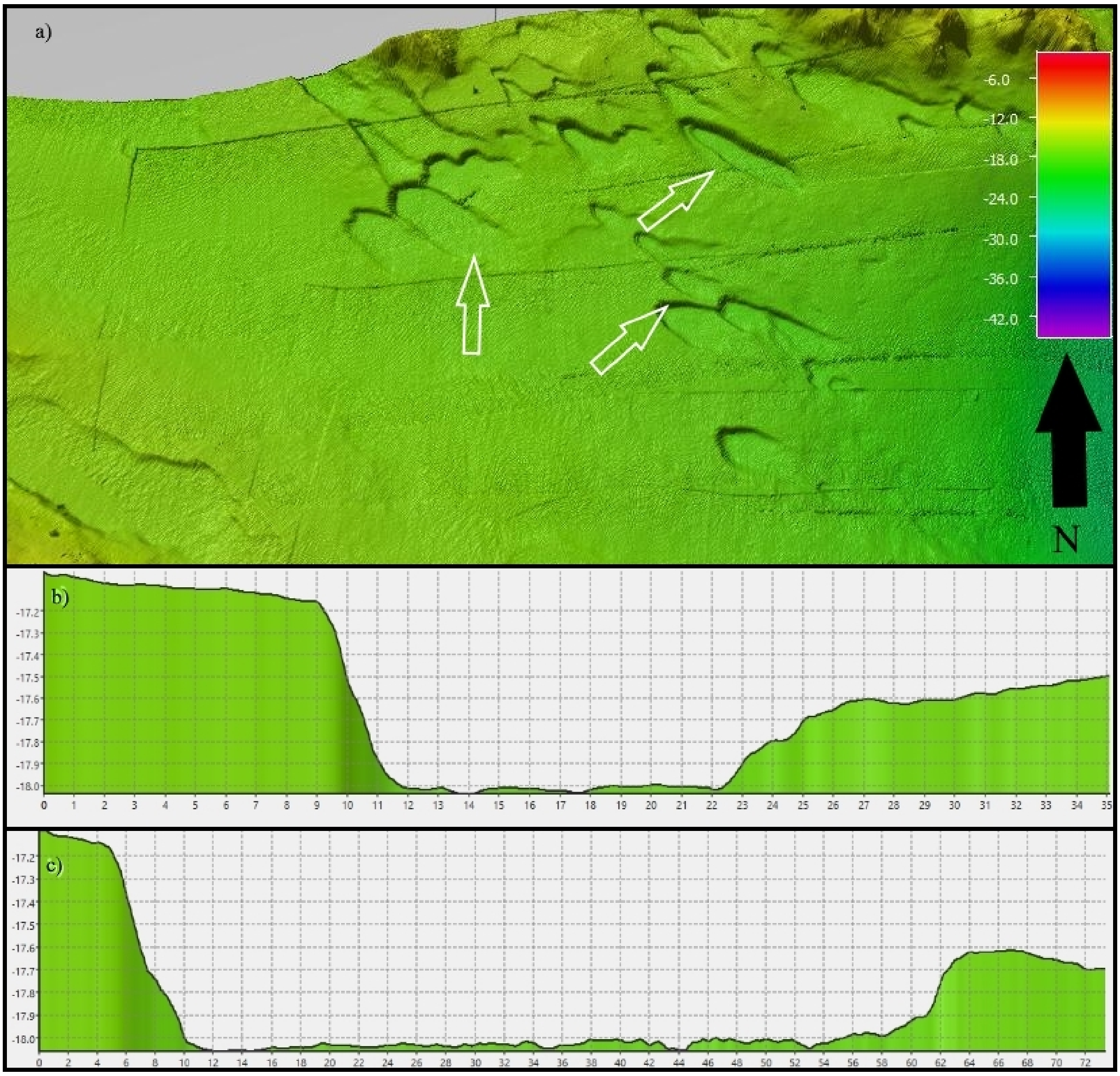


Figure (17). Overhead view of 22 elliptical egg shaped features on the sea floor at depths of about 17 m to 18 m. b) shows a cross section of the short axis while c) shows the long axis cross section. The cross sections both reveal that the north-west end is about 1 m high and the south-east end is about 0.5 m high.

The water column data representing the area is seen in table (4).

| SBP Profile | Multibeam tracks | Map |
|---|---|---|
| 20130904_114640<br>20130904_092941<br>20130904_125107<br>18311424 | 0087_20130831_153123<br>0088_20130831_155336<br>0089_20130831_162240<br>0090_20130831_164910<br>0091_20130831_171231 | 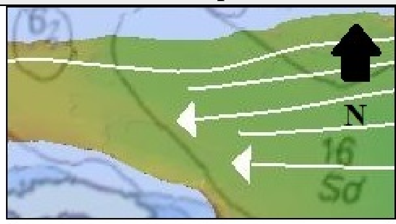 |

Table (4). SBPs with their corresponding multibeam tracks. The multibeam tracks can be seen in the Map as taken from the north most squared area in figure (6).

The result of water column data re-projected into Fledermaus is shown in figure (18). While no features of note were seen across the steps in figure (16) the data over the egg-shaped features do show a few elongated features originating from the sea floor features and stretching to the sea surface, see figure (18).

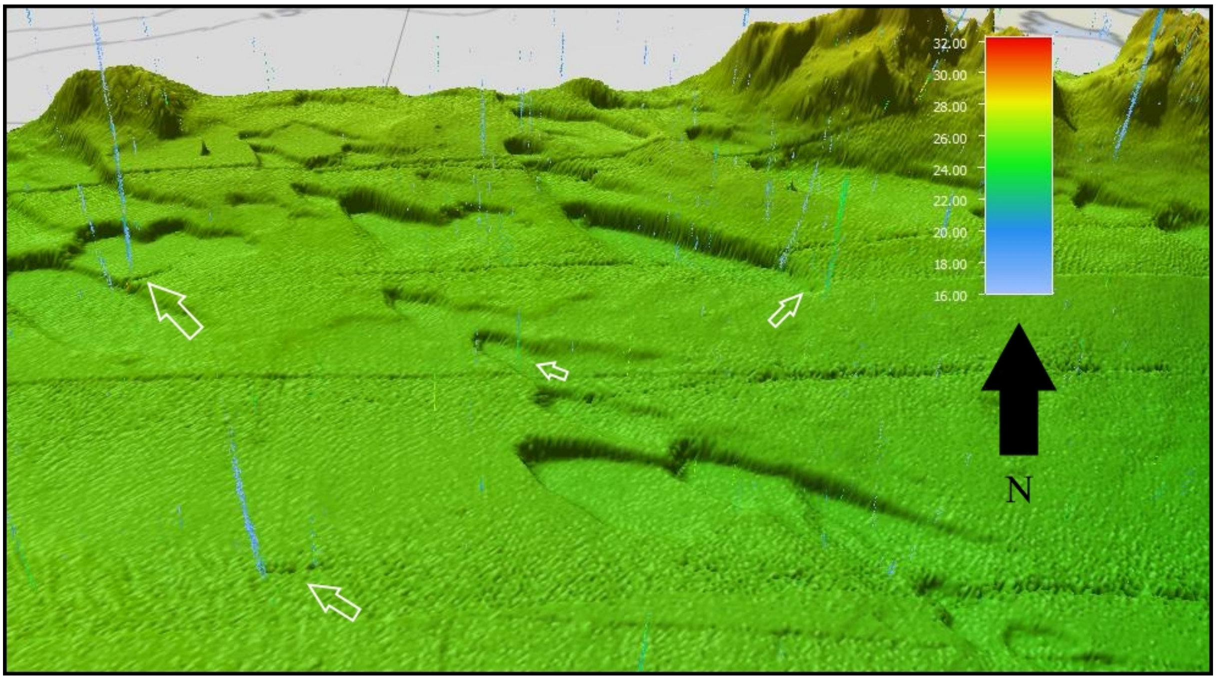


Figure (18). Fledermaus view of features originating from the sea floor near the egg-shaped features. The arrows added picks out a handful of visible features.

### 3.2.2 Sub-Area 2

The multibeam of sub-area 2 show multiple crescent shaped features south of the small island Skåren and the features lie from about 9 m to 13 m depth and facing north-west and south-eastly direction. Most of them are at a 70° slope facing south-east, see figure (19) and (20). The blanked-out areas such as the Skåren Island parts are land mass or too shallow areas for the research vessels to survey.

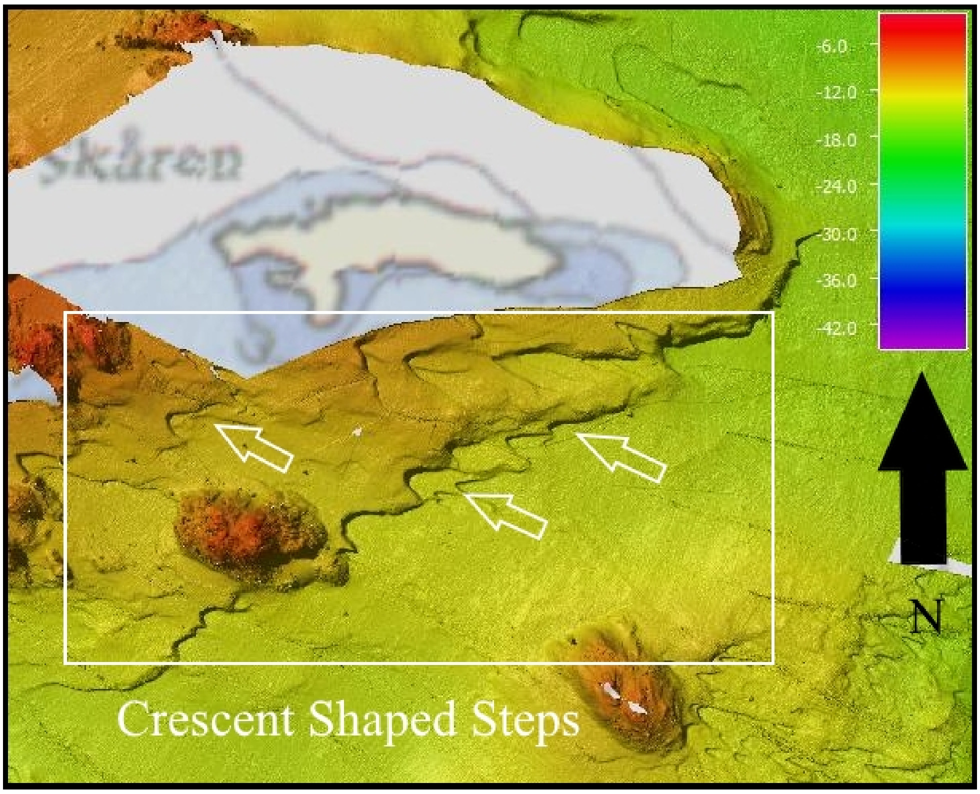


Figure (19). Multiple crescent shapes can be seen south of Skåren in the white box. These are relatively shallow compared to the shapes seen in sub-area 1. The unmapped areas are the Skåren Island and bedrock outcrop which are out of reach for the RVs.

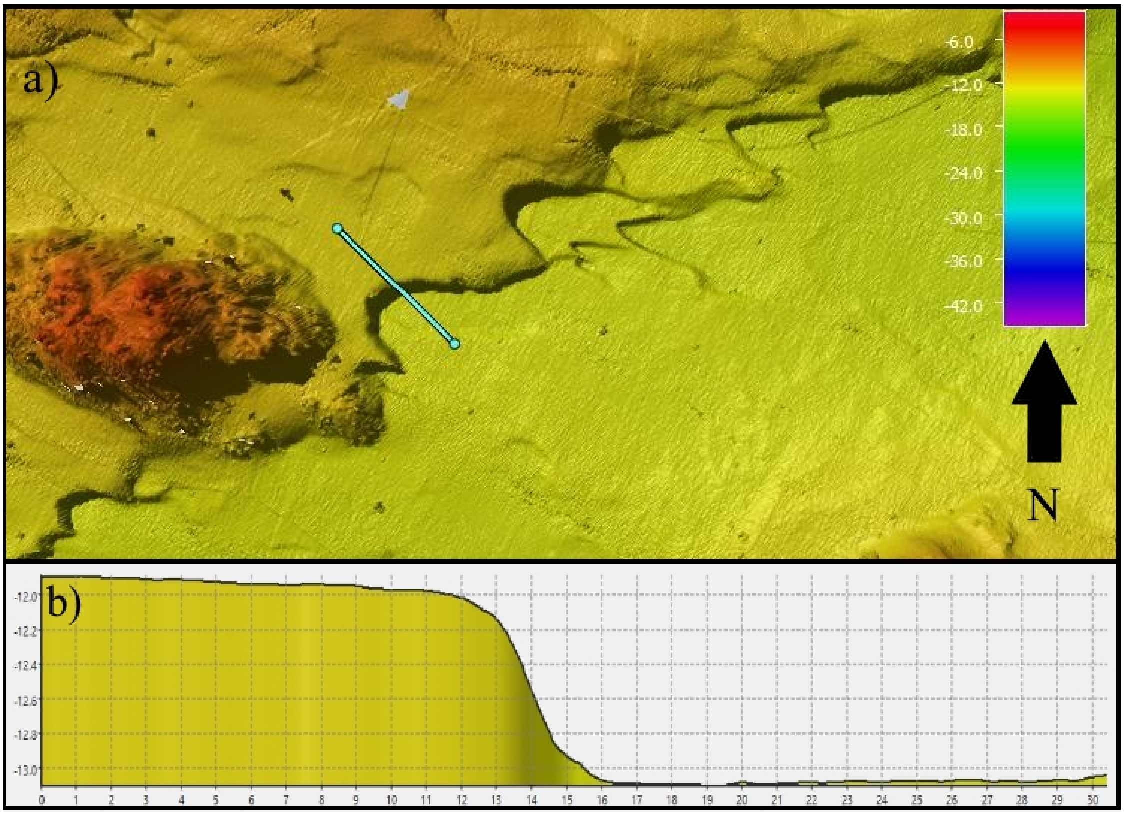


Figure (20). Crescent features in a) and the corresponding profile in b) shows that the step is 1 m high and has a relatively steep slope of about 70°.

For the water column table (5) show the corresponding SBP in the area along with the multibeam tracks. A total of five multibeam tracks were used in FMMidwater and processed with the feature detection tool. The water column data does reveal features coming from the crescent steps at about 13 m depth and rising towards the surface, see figure (21).

| SBP Profile | Multibeam tracks | Map |
|---|---|---|
| 20130904_090928 | 0058_20130831_112420<br>0059_20130831_114504<br>0063_20130831_121917<br>0064_20130831_124121<br>0065_20130831_130254 | 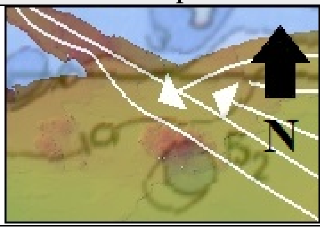  |

Table (5). The map shows sub-area 2 with which SBPs are used. Multibeam track lines in white which is also where the water column data is represented.

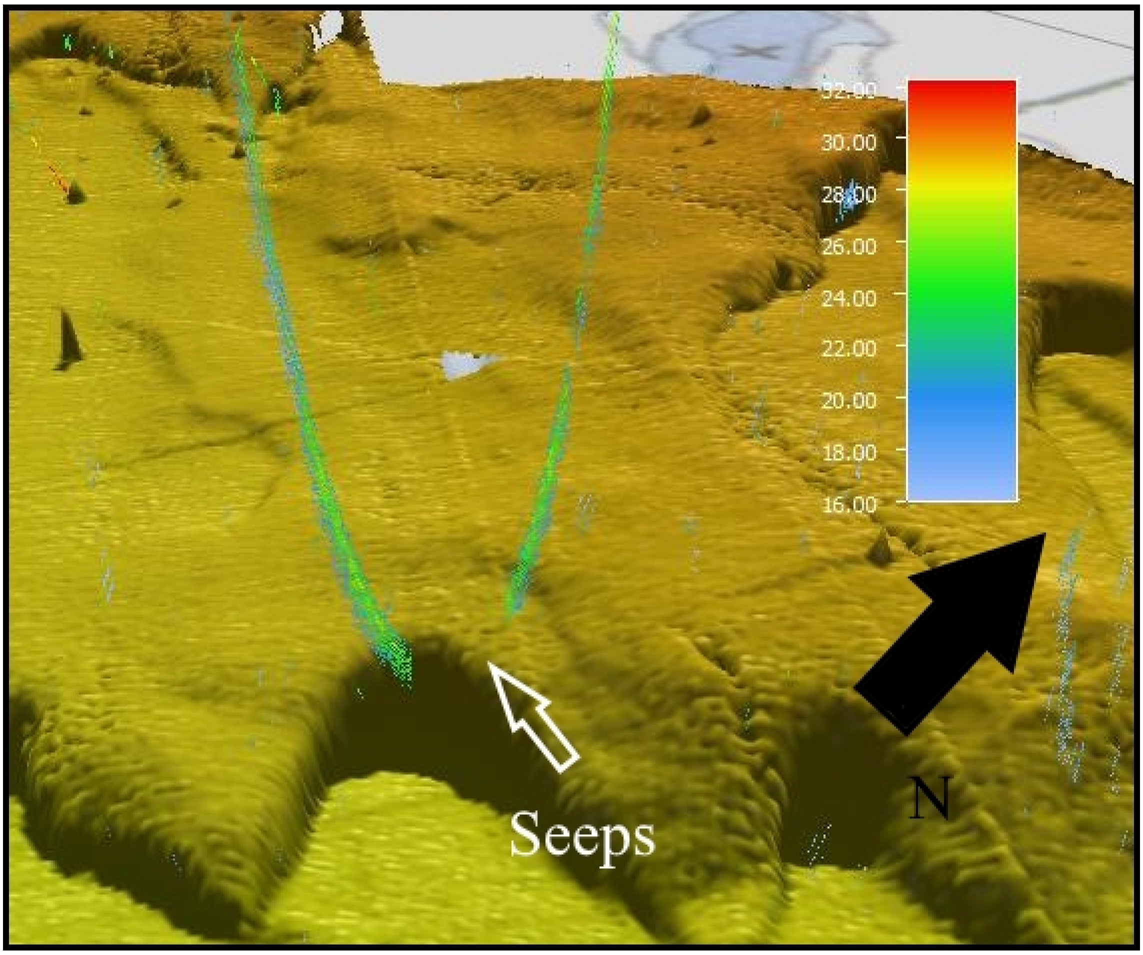


Figure (21). Seep rising from the edge of a crescent step as seen in the water column data in Fledermaus.

### 3.2.3 Sub-Area 3

The multibeam survey in sub-area 3 reveal two pairs of steps almost parallel to each other. Separated by an outcrop they are both approximately 100 m long from step to step, figure (22). They appear at about 14 m depth and both ending with a new step at about 15.5 m depth.

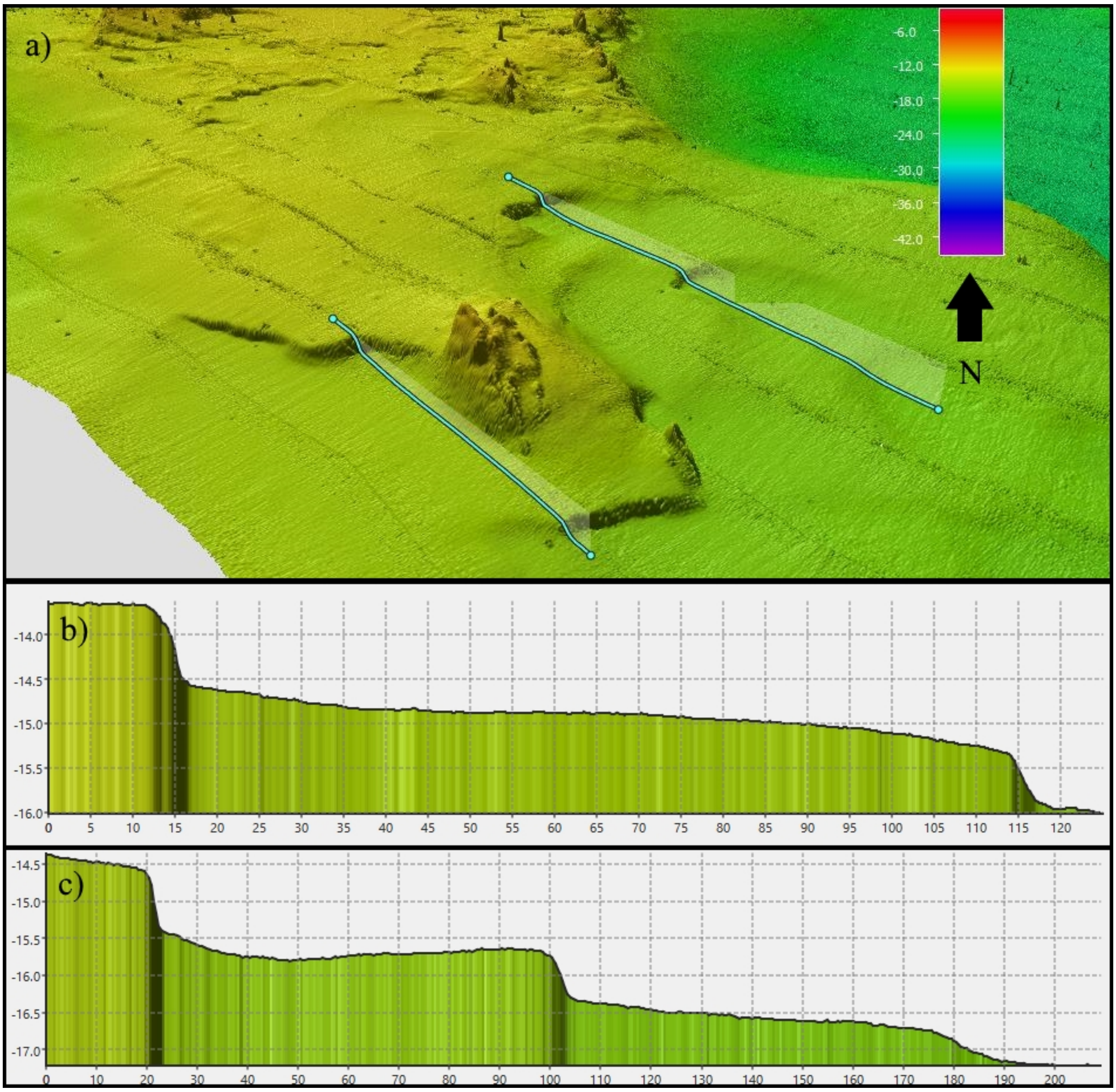


Figure (22). Shows four distinct steps in the multibeam data in a). b) shows the step furthest to the north and c) is closes to the camera. Both steps are ~1 m high and there is ~100 m between the steps in both b) and c). Difference in steepness though since the lowest step in b) has a slope of ~45° and c) has ~70° slope.

A total number of five multibeam profiles were used in the FMMidwater software for sub-area 3 see table (6). As in previous sub-areas the tracks were chosen near the SBPs taken in the sub-area.

| SBP Profile | Multibeam tracks | Map |
| --- | --- | --- |
| 20130904_084807<br>20130904_105339<br>29051049 | 0035_20120902_111518<br>0036_20120902_113724<br>0037_20120902_115940<br>0026_20120902_085613<br>0028_20120902_094655 | 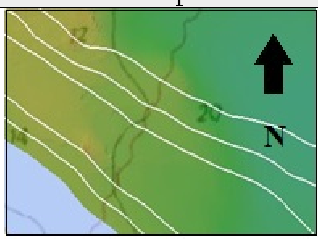 |

Table (6). The map shows sub-area 3 with which SBPs are used. Multibeam track lines in white which is also where the water column data is represented.

The water column data did show some features in the column rising towards the surface but only at one at each step which in both cases were the shallower one. In figure (23) the features can be seen.

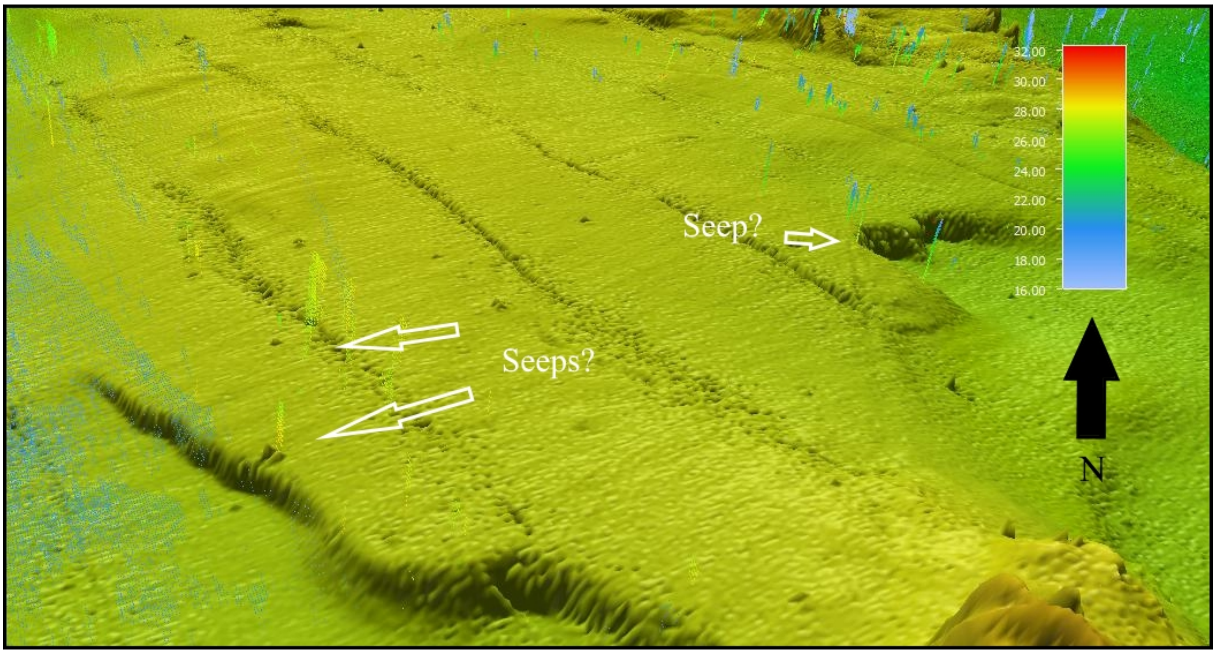


Figure (23) Multibeam surface with water column data above the steps. The water column data in both a) and b) show features in the water column.

# 4. Interpretation and Discussion

## 4.1 Interpretation of Geophysical Data Sub-Area 1

The lithological unit I does not seem to be laminated whereas units II-VI show an alternation between strong and weak reflections. This is likely the varved glacial clay described in Andrén et al. (2011), although the acoustic lamination is not reflecting the individual varves due to the limited vertical resolution, and the unit I being postglacial unlaminated clay. Steps and bowls in the area seem to be found in units I and II, the top sediments so perhaps the sediments here are less compacked. In figure (9) the steps seem to follow unit III closely but not cutting trough. This could indicate that units III and below are less porous and harder to erode. Gas blanking is widely prominent in all units and in the deep areas postglacial sediment with gas seems to be accumulating (figure 9). Figure (16) and (17) show the crescent shaped steps and egg shaped bowls seem to be clustered at a water depth of about 12 m and 18 m in the sub-area 1. The steps also seem to be close to land like the island Skåren. They look

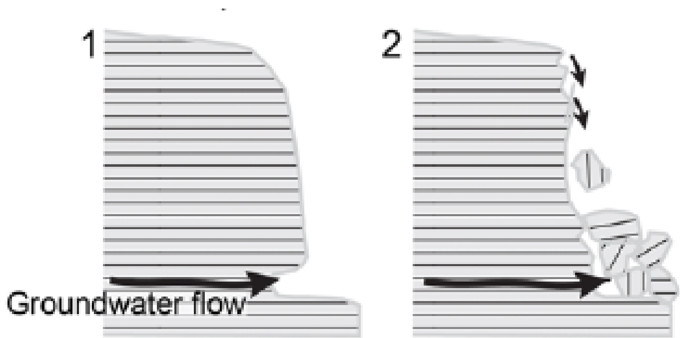


Figure 24. Conceptual model of step formation from Jakobsson, et al. (2012). This shows laterally flowing groundwater causing undermining (1) with subsequent collapse (1).

similar but as stated in the results section the slope of the steps to the north-east there are egg shaped bowls seem to be clustered at a water depth of about 12 m and 18 m in the sub-area 1. The steps also seem to be close to land like the island Skåren. They look similar but as stated in the results section the slope of the steps to the north-east there are egg shaped rather than crescent shaped. The egg shapes are found in deeper waters at around 18 m and look like the "Sundsbådarna pockmarks" described by Söderberg & Flodén (1997). The steps found in shallower waters closely resemble the steps in Jakobsson, et al. (2016) where the explanation behind the steps were undermining of the overlying sediments resulting in collapse, see explenation model in figure (24).

The deformation lenses that are originating from the acoustic basement and could be an indicator of seepage but looking at some of the cases the sediments are mirroring the acoustic basement topography (draping) instead. Some of the deformations cannot be explained with draping and they are also diffuse. Research from Ergün et al. (2002) and Canet, et al. (2010) explains similar deformation columns as escaping gas in the sediments causing the deformation and blanking. Here however not all the lens columns are blanked out but rather diffuse, making gas blanking less likely to cause the blurriness.

Through the water column data over the elliptically-shaped features we can see seeps originating from the features. The seeps are visible due to a strong impedance difference between the water and the features (Schneider von Deimling, et al., 2007). The features are therefore interpreted as gas, which is supported by the chirp sonar profiles since gas blanking and turbidity can be seen in the sea floor. The bowls can be interpreted as pockmarks when combining the SBP and multibeam data. These observations further enable the interpretation that the pockmarks in sub-area 1 are created from gas release. The generation of the pockmarks could be like the description in O'Regan, et al. (2015). Perhaps the crescent shaped steps were once like the pockmarks but has partly been eroded away. Jonsson et al. (2003) stated that the seafloor in this area is more prone to erosion because of currents and isostatic rebound. So a prolonged erosional process could have created crescent steps, see figure (24). The steps could have been at the depths in of the pockmarks but perhaps longer isostatic rebound brought the pockmarks higher up the water column making them more exposed to erosion such as wind and wave erosion. If we have sea floor rise due to isostatic rebound then perhaps this could contribute to pockmark collapse forming steps. This could explain the more gentle slope in some of the steps. The materials here would collect downslope causing the 45° steps seen. As mentioned, the chirp sonar profiles shows signs of gas in the sediment column. In figure (10)

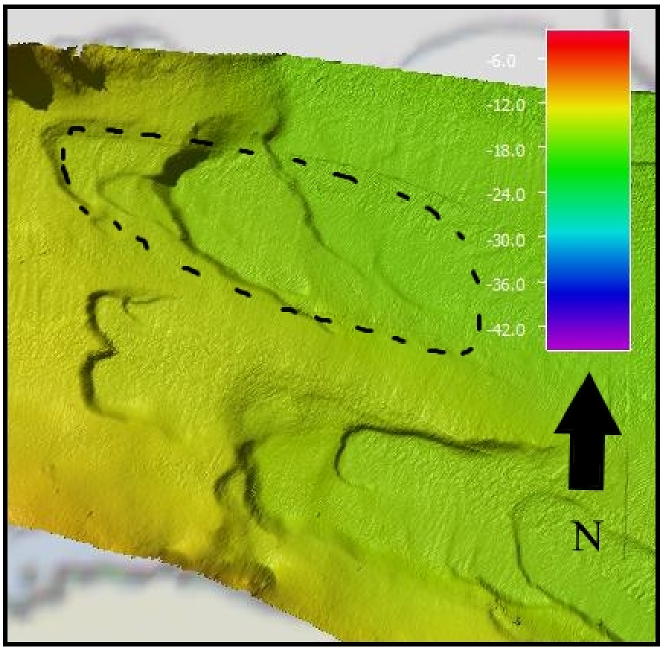


Figure 25. Example how a big pockmark could have been a precursor to the crescent shaped steps before erosion.

there appears to be a discontinuity in the sediment layer acocompanied by gas blanking. The blanking seems to strech from deep down the sediments. This could be caused by a violent release of gas that has built up from bedrock seeps being trapped under a less permeable layer of sediment (units III-VII).

### 4.2 Interpretation of Geophysical Data Sub-Area 2

The crescent like features around the Island Skåren are gathered around the south of the island. Using the SBP from the area it does have the step feature that were found in Söderberg & Flodén (1997) and Jakobsson, et al. (2016). The one SBP in the area (figure 14) show extensive blurring underneath which could be gas blanking. The blanking also occurs close to the acoustic basement further south-west in the profile. This could indicate that whatever is causing the blanking is emerging from the basement. Deformation of the layers can just about be seen due to the blanking and seem to correlate with the blanking. Draping is not the interpreted cause here since the layers further south-west does not exhibit draping even with changing bottom topography. There is no chirp sonar profile that shows the subsurface beneath the water column seeps seen in figure (21) unfortunetly. However, hydroacoustic studies from Canet et al. (2010), Greinert, et al. (2010) and Jones, et al. (2010) interprete similar seeps as methane gas escape. The intense blanking under the sea floor at the SBP is roughly 150 m away leading to the possible interpretation that this is a gas seep. Water is a possibility though, the water could recharge at Skåren and be transported from the land under the water via less permeable layers like the strong reflector in figure (25) below.

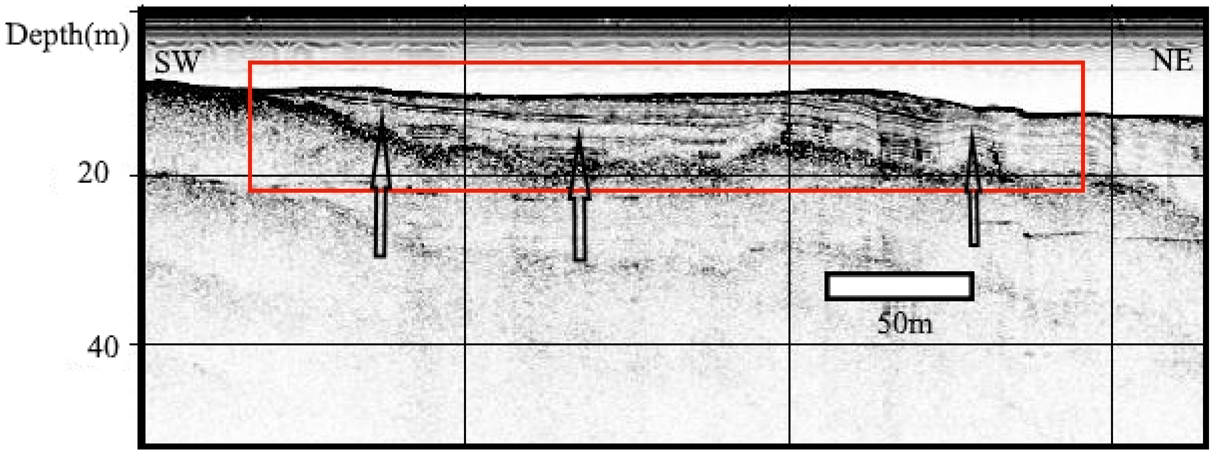


Figure (26). Profile 20130904_090928 particularly strong reflectors traced along the sea floor which starting from acoustic basement.

The strong reflectors traced through the sediments seems to stop around the step. The seep captured in this study (figure 21) shows that seeps are happening today and it is not a ceased activity.

### 4.3 Interpretation of Geophysical Data Sub-Area 3

The steps here have the same characteristics as described in Söderberg & Flodén (1997) and Jakobsson, et al. (2016). The sediment profiler revelal convexly deformed lens like layers underneath and in close proximity to the steps, and tracking the deformation downwards leads to the acoustic basement as seen in figure (12). Looking at figure (12) the deformation cause could be originating from the basement and could be interpreted as gas or other fluid traveling up the sediments in the fashion described by O'Regan, et al. (2015). In some areas though, the sediment layers could be the result from sediment follwing the seafloor topography forming a drape. This does not seem like the case in all of the deformation lenses, but in figure (13) there is prominent draping, whereas there's less prominent draping in figure (12). Changes in the topography there does not seem to contribute to the lens formation. It is not clear if the process is ongoing or if the steps are remnants of old fluid erosional processes. There is little signs of gas blanking and turbidity in figure (12) making a liquid fluid a more likely candidate. In figure (12) the deformation seems to halt at a certain layer and maybe the fluid could have traveled laterally hitting a more permeable layer and then escaping, creating collapse in the process.

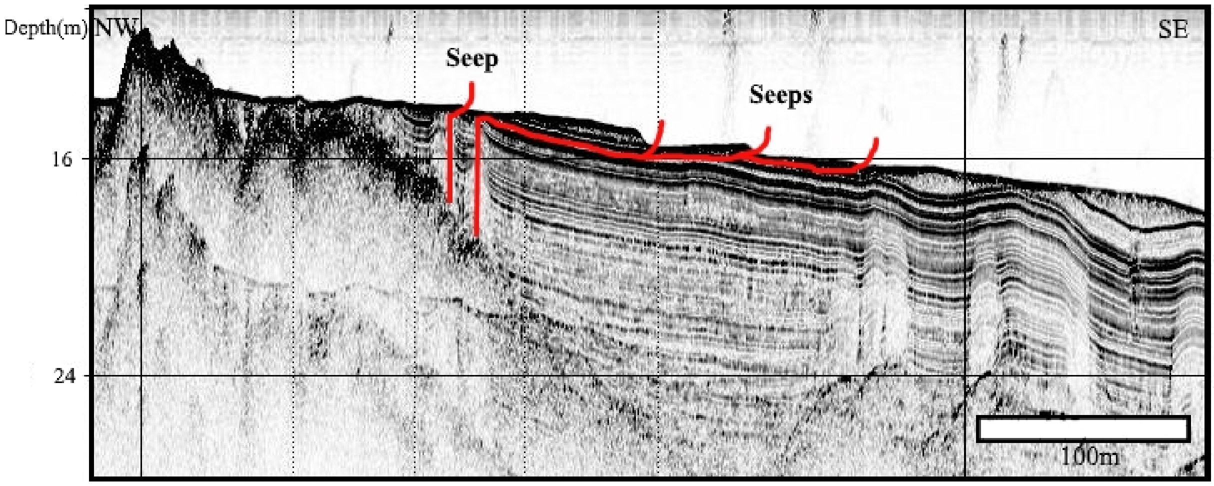


Figure (27). Showing profile 20130904_084807. The deformation of sediments to the left seems to stop at the red layer that seems to be less permeable that the other layers. The red lines marks where fluids could have travelled first vertically and then laterally through some layer and finally beeing able the escape through units (I or II). The eroded sediments makes tracking the sediment difficult.

In figure (27) is an interpretation of figure (13) attempting to show possible fluid paths in the sediments. As seen in the figure the steps form after the glacial layers and are formed under or in the post glacial clay. The difference here from figure (25) is that this figure demonstrates a formation process suggested in Jakobsson, et al. (2016). The deformation seems to have stopped at a less permeable layer and could have diverted the fluid laterally. However, the strong reflector at the sea floor makes it difficult to see any other layers close to the sea floor. The multibeam and water column combination is shown to complement the interpreted SBP profile from figure (13) where we can see some features in the water around the steps. This can be small seeps of fluid that rises towards the surface before being mixed into the seawater. The chirp sonar profile (figure 14) show diffuse features in the waters above the steps but the strong reflector at the sea floor makes it difficult to see if the feature could originate from the seafloor.

### 4.2 Formation

#### 4.2.1 Groundwater Escape

The landforms described in Söderberg & Flodén (1997) and Jakobsson, et al. (2016) closely resemble the landforms found in this study. The sediments mentioned by Jakobsson, et al. (2016) look like the lens columns in figure (13) and has been attributed to escaping groundwater. Comparing these with the gas blanked sediments in Ergün et al. (2002) the ones in figure (13) are very visible wheras the columns in Ergün et al. (2002) are entirely blanked out. If it is indeed groundwater, some possible explanations for seeps are presented below.

An explanation model behind the features could be as described by (Post, et al., 2003). During glacial periods the exposed shelf is flooded with fresh glacial water and meteoric water which is recharged into the shelf sediments, pushing the saline water out into the sea. During interglacial periods the pressure from the surrounding ocean with rising sea level pushes the saline waters inwards and stops the expansion of fresh waters. The water is preserved in the shelf sediments if it has passed a less permeable layer which allows for storage. This explanation applied to the study area water from the melting ice sheet during the beginning of Yoldia sea stage or during the Ancylus Lake stage could permit fresh water recharge into the sediments.

The area was losing ice after the time of drainage of the Baltic Ice Lake BP (Andrén et al., 2011). The sea level record by Berglund (2012) and records and model results from Lambeck, et al. (1998) show that the study area has area has not been subareally exposed for about 10000 years, i.e. since the the Ancylus sea stage. As the passage to Kattegat opened through Öresund and Great Belt during the Littorina Sea stage the salinity increased (Andrén et al., 2011) and the more saline waters pushing on the fresh pore waters which could cause the fresh water to rise from the sediments.

In the areas where the steps are some distance from the deformed layers as in figure (11) and (13) the water an explanation model could be that the fluids travel laterally until reaching a more permeable sediment layer to escape from, as described in (Church, 1996). This could be the case in sub-area 1 and 2 since many steps appear around the Island Skåren. Water could recharge at Skåren and travel outwards until encountering a more permeable layer allowing for escape as explained in figure (26). From SGU terrestrial soil maps (appendix I), most of the landmass is bare bedrock with sparse areas of glacial clay, sand and sandy moraine Recharge of groundwater in the area could be through cracks in the bedrock. The hydraulic conductivity would be on the order of 10 m/day (if the bedrock is fractured) to $10^{-7}$ m/day (if unfractured) (Heath, 1987). The bedrock conductivity could mean that a large volume of water would flow out into the sea from land, which could have ramifications if the water carries terrestrial nutrients.

The geological bedrock map from SGU (see appendix I) show one deformation zone in the study area. There is a synform cutting diagonally from north-west to south east in parallel with the deformation, which can also be seen in figure (6a) as the deepest parts of the study area (purple colour coding). A possibility could be that cracks in the crystalline bedrock under the marine sediments enables ground water seeps out through the sediments.

#### 4.2.2 Gas Seepage

A possible explanation to the features is the seepage of methane gas. Methane emerging from the sea floor is not uncommon in the Baltic. Sub-bottom profiles from studies in other oceans (e.g. Gay et al. 2007, Vardar & Alpar (2016)) show that pockmarks are present around gas seeps. They also resemble the step features in this study (because a step feature could be described a pockmark with one side missing). Surveys by Söderberg & Flodén (1992) in the Stockholm archipelago investigating pockmarks has revealed seepage of thermogenic gas from near tectonic lineaments. The gas travel upwards through glacial and postglacial sediment through permeable layers. The origin of the gas could come from inside the earth (abiogenic gas), decayed material deep inside the sediment (biogenic gas) or possibly gas that travels in the groundwater Söderberg & Flodén (1992). However, it should be noted that no gas signatures were detected in the chemical analysis of the clays that was collected near the pockmarks in the study by Söderberg & Flodén (1997). Another explanation for gas seep is offered in Söderberg & Flodén (1992), who suggest that the gas is released from crystallization processes in the crust or groundwater flow through the bedrock that carries gas in the water. Looking the SGU bedrock map we can see the bedrock has been faulted and fractured and therefore can enable the formation of gas seepage as described in Söderberg & Flodén (1992). The features in the study area could be explained by gas seepage if methane signals are found in the sediments. Signs of gas were prominent in the form of blanking and acoustic turbulence. The sediments furthest down the sediment column (sedimentary units III-VII) in this part of the Baltic Sea are from the Baltic Ice Lake stage and contain low amounts of organic materials, according to Andrén et al. (2011). The gas could be originating from the bedrock if not from the lower sediment units.

As mentioned, the features in sub-area 1 could be eroded pockmarks, figure (20). Because there are no geochemical data this cannot be conclusively determined and the formation via ground water seeps an also not be concluded. However, similar deformed columns of diffuse reflectors have been seen in studies by Ergün et al. (2002) and Canet, et al. (2010) who has concluded that the columns are formed by escaping gas. The features left behind after escaping gas show step and bowl shaped pockmarks. Sub-area 2 show two long columns in the water column at one of the steps which could be escaping gas as the sediments below show gas blanking and diffuse columns. Sub-area 3 shows minor seeps from the sea floor with SBPs showing gas blanking in all the profiles except the one in figure (13). The more diffuse columns might be columns with more gas concentration whereas the columns with less diffuse layers could contain less gas. The formation process in Jakobsson et al. (2016) could still be aplicable if the gas encounters a less permiable sediment layer making it travel laterally. This could possibly cause porosity loss due to gas bubbles. and subsequent collaps of overhangning sediments.

### 4.3 Implications for Ground Water Formation

The difference in formation process can have environmental consequences. If the assumption is made that the steps are formed from groundwater seepage, and the process is ongoing today, it could be a factor worsening the eutrophication problem. The eutrophication problem in the Baltic is caused by overall low oxygen concentration and excess nutrients delivered by overland water flow (Andersen, et al., 2010). But ground water might be an underestimated source of nutrients. As groundwater seeps into the brackish waters of the archipelago and since groundwater movement is determined by topography it can be concluded that the closest recharge of groundwater takes place on the islands or coastal areas. On land, precipitation in areas of farming and industry could carry nutrients and pollutants into the ocean. The lack of oxygenin the Baltic Sea is caused by the narrow straits connecting the Baltic Sea to the North Sea limiting the renewal by oxygen-rich Atlantic sea water.

Terrestrial nutrient sources can come from fertilizing of farmland, human hygiene and industry. With the nutrient transport to the sea it allows for increased phytoplankton productivity. When the plankton die, the biomass accumulates on the sea floor, and the process of decomposing the biomass requires oxygen. At some point the oxygen levels are depleted leaving behind dead bottoms leading to loss of fauna (Pawlak, Laamanen, & Andersen, 2009). The reports by Pawlak, et al. (2009) and Andersen, et al. (2010) makes no mention of groundwater as a pollutant source. The eutrophication potential of groundwater seeps in marine environments needs to be much better understood, and should be a focus of future research.

### 4.4 Future Research

If the assumption is made that the step features are created by ground water seepage, then if the water comes from neighbouring land sources with agricultural activity. The eutrophication problem in the Baltic could therefore have a previously overseen source. To determine the origin of the steps found in this study the following is suggested for future research. Geochemical tracer studies looking at e.g. hydrogen, oxygen, radon have been a proven method for tracking the origins of groundwater seeps in marine environments (Kiro, et al, 2015 & Zhang & Satake, 2003). The gas seepage question can also be investigated using carbon isotope fractioning as done by Söderberg & Flodén (1992).

The geophysical methods used to look in to the sediments works for soft sediments the acoustic methods here might not be sufficient when investigating the bedrock. As mentioned gas can seep through cracks in the bedrock and these cracks cannot be fully realised with the methods used in the study. To map the bedrock high frequency seismic methods should be used. The use of airguns can generate a frequency between 50-100 kHz and can be used for a bedrock profile in search for tectonic lineaments (Jones, 1999). New surveys with the same equipment used in this study could show if there are any changes in bottom topography since the last survey. If there are no differences then maybe the erosional process behind the step features down or stopped entirely. New surveys could cover the areas with no multibeam data which would complement the SBP data which was analysed in this project.

Petrophysical well logging or core logging could provide further understanding of the study area. With a resistivity log a distinction between salt water and sea water could be possible since fresh water has higher resistivity than salt water (Rider & Kennedy, 2011). A porosity log could reveal a loss of porosity which allows for fluid migration since porosity should decrease with depth as sediments compact (Rider & Kennedy, 2011). An acoustic log could spot the differences in salt water and fresh water velocities also this kind of log can also be used with porosity logs to correlate the two properties. The resulting plot can be used to find areas where porosity and p-wave velocity drops (Rider & Kennedy, 2011). The precense of gas can also be seen in well logging when plotting neutron porosity and bulk density a seperation apperars as an increase in porosity and loss in bulk denisty (Rider & Kennedy, 2011).

## 5. Conclusion

The goal of this project was to interpret and analyse step-like sea floor features of Asköfjärden, by processing and interpreting existing marine geophysical data. Based on interpretation of multibeam bathymetry, chirp sonar profiles and multibeam water column data, the following conclusions can be made.

- Several step-like features in the form of crescents and oval depressions were found in acoustic units I and II of post glacial clay with one exception where the steps seem to be in unit III (glacial clay). The water column data reveal what could be fluid seeps above both features and the sediment layers beneath the features show fluids migrating. Signatures of gas are present in the form of gas blanking and acoustic turbidity. There are signs of other fluids present that does not show gas signatures.
- A possible formation mechanism is fluid flowing laterally either originating from land or in deeper sediment layers causing undermining of overlying sediments. But the composition of the fluid is not the same in all the cases when looking at acoustic signatures. Previous studies have attributed groundwater as the fluid with these signatures.
- The oval pockmarks closely resemble the steps. The sediments under the pockmarks show gas blanking and seeps can be seen in the water column, therefore the pockmarks are probably from gas seeps. The steps look like a pockmark cut in half and the pockmarks could be preludes to the steps and is formed from erosional processes in Asköfjärden.
- Deformed lenses of sediment resembling a column are faded or blanked which could point to fluid traveling vertically. But this could be the sediments following the bottom topography which is draping rather than layers deformed by fluids pushing upwards.
- The formation of the steps found in Asköfjärden cannot be determined from acoustic measurements alone. The fluid migrating the sea floor could be both gas and groundwater.
- The eutrophication of The Baltic Sea is a problem and if the steps are made from groundwater seeps this could be an overseen source of nutrients. If the groundwater seeps from the sediments has a terrestrial source nutrients from farming or industry could find its way into the Baltic and further enable eutrophication.

## 6. Acknowledgements

First I would like to thank my supervisors Richard Gyllencreutz and Martin Jakobsson for all the help and guidance they provided. As a bachelor student, any time and attention given from lecturers and professors is a treat.

Lastly a thank you to everyone that showed interest in my work or had a word of encouragement during the work on this thesis.

## 7. References

Andersen, J. H., Korpinen, S., Laamanen, M., Wolpers, U., Claussen, U., Durkin, M., . . . Zweifel, U. L. (2010). *Ecosystem Health of the Baltic Sea: HELCOM Initial Holistic Assessment.* Helsinki: Helsinki Commission.

Andrén, T. U., Björck, S., Andrén, E., & Zillén, L. (2011). The Development of the Baltic Sea Basin During the Last 130 ka. i J. Harff, *The Baltic Sea Basin, Central and Eastern European Development Studies* (ss. 75-97). Berlin: Springer-Verlag.

Berglund, M. (2012). Early Holocene in Gästrikland, east central Sweden: shore displacement and isostatic recovery. *Boreas*, 263–276.

Björck, S. (2008). The late Quaternary development of the Baltic Sea. *Assessment of climate change for the Baltic Sea Basin*, 398-407.

Canet, C., Prol-Ledesma, R. M., Dando, P. R., Vázquez-Figueroa, V., Shumilin, E., Birosta, E., . . . Tauler, E. (2010). Discovery of massive seafloor gas seepage along the Wagner Fault, northern Gulf of California. *Sedimentary Geology*, 292–303.

Church, T. M. (1996). An underground route for the water cycle. *Nature*, 579-580.

Davis, A. M. (1992). Shallow Gas: An Overview. *Continental Shelf Research*, 1077-1079.

Ergün, M., Dondurur, D., & Cifci, G. (2002). Acoustic evidence for shallow gas accumulations in the sediments of the Eastern Black Sea. *Terra Nova*, 313–320.

Gay, A., Lopez, M., Berndt, C., & Séranne, M. (2007). Geological controls on focused fluid flow associated with seafloor seeps in the Lower Congo Basin. *Marine Geology*, 68–92.

Greinert, J., Lewis, K., Bialas, J., Pecher, I., Rowden, A., Bowden, D., . . . Linke, P. (2010). Methane seepage along the Hikurangi Margin, New Zealand: Overview of studies in 2006 and 2007 and new evidence from visual, bathymetric and hydroacoustic investigations. *Marine Geology*, 6–25.

Heath, R. C. (1987). *Basic Gorund-Water Hydrology*. Denver: U.S. Geological Survey.

Jackalin, M. (den 6 Maj 2017). *Stockholm University* . Hämtat från Östersjöcentrum: http://www.su.se/ostersjocentrum/ask%C3%B6laboratoriet/m%C3%A4tboj

Jakobsson, M., Björck, S., Alm, G., Andrén, T., Lindebergd, G., & Svensson, N.-O. (2007). Reconstructing the Younger Dryas ice dammed lake in the Baltic Basin: Bathymetry, area and volume. *Global and Planetary Change*, 355–370.

Jakobsson, M., Gyllencreutz, R., Mayer, L., Dowdeswell, J., Canals, M., Todd, B. J., . . . L., L. R. (2016). Mapping submarine glacial landforms using acoustic methods. In J. Dowdeswell, M. Canals, M. Jakobsson, B. J. Todd, E. K. Dowdeswell, & K. A. Hogan, *Atlas of Submarine Glacial Landforms: Modern, Quaternary and Ancient* (pp. 17-40). London: The Geoloical Society.

Jakobsson, M., O'Regan, M., Gyllencreutz, R., & Flodén, T. (2016). Seafloor terraces and semi-circular depressions related to fluid discharge in Stockholm Archipelago, Baltic Sea. i J.

Dowdeswell, M. Canals, M. Jakobsson, B. J. Todd, E. K. Dowdeswell, & K. A. Hogan, *Atlas of Submarine Glacial Landforms: Modern, Quaternary and Ancient* (ss. 305-306). London: The Geological Society.

Jones, A., Greinert, J., Bowden, D., Klaucke, I., Petersen, C., Netzeband, G., & Weinrebe, W. (2010). Acoustic and visual characterisation of methane-rich seabed seeps at Omakere Ridge on the Hikurangi Margin, New Zealand. *Marine Geology*, 154–169.

Jones, E. J. (1999). *Marine Geophysics.* Chichester: John Wiley & Sons Inc.

Jonsson, P., Persson, J., & Holmberg, P. (2003). *Skärgårdens bottnar: En sammanställning av sedimentundersökningar gjorda 1992–1999 i skärgårdsområden längs svenska ostkusten.* Trelleborg: Naturvårdsverket.

Judd, A., & Hovland, M. (1992). The evidence of shallow gas in marine sediments. *Continental Shelf Research*, 1081-1095.

Kiro, Y., Weinstein, Y., Starinsky, A., & Yechieli, Y. (2015). Application of radon and radium isotopes to groundwater flow dynamics: An example from the Dead Sea. *Chemical Geology*, 155–171.

Lambeck, K., Smither, C., & Johnston, P. (1998). Sea-level change, glacial rebound and mantle viscosity for northern Europe. *Geophysics*, 102–144.

Lundqvist, J., Lundqvist, T., Lindström, M., Calner, M., & Sivhed, U. (2011). *Sveriges Geologi: från urtid till nutid.* Lund: Studentlitteratur.

Lurton, X. (2010). *An Introduction to Underwater Ahoustics: Principles and Applications.* Berlin: Springer.

Mosher, D. C., & Simpkin, P. G. (December 1999). Status and Trends of Marine High-Resolution Seismic Reflection Profiling: Data Acquisition. *Geoscience Canada*, ss. 174-188.

Nichols, G. (2009). *Sedimentology and Stratigraphy.* Oxford: Wiley-Blackwell.

O'Regan, M., Forwick, M., Jakobsson, M., Moran, K., & Mosher, D. (2015). Seafloor cratering and sediment remolding at sites of fluid escape. *Geology*, 895-898.

Pawlak, J. F., Laamanen, M., & Andersen, J. H. (2009). *Eutrophication in the Baltic Sea: An integrated thematic assessment of the effects of nutrient enrichment in the Baltic Sea region.* Helsinki: Baltic Marine Environment Protection Commission.

Post, V. E., Groen, J., Kooi, H., Person, M., Ge, S., & Edmunds, W. M. (2003). Offshore fresh groundwater reserves as a global phenomenon. *Nature*, 71-78.

Rider, M., & Kennedy, M. (2011). *The Geological Interpretation of Well Logs.* Glasgow: Rider-French.

Robb, J. M. (1984). Spring sapping on lower continental slope, offshore New Jersey. *Geology*, 278-282.

Schneider von Deimling, J., Brockhoff, J., & Greinert, J. (2007). Flare imaging with multibeam systems: Data processing for bubble detection at seeps. *Geochemistry Geophysics Geosystems*, 1525-2027.

Schock, S. G., LeBlanc, L. R., & Mayer, L. A. (1989). Chirp subbottom profiler for quantitative sediment analysis. *Geophysics*, 445-450.

Stroeven, A. P., Hättestrand, C., Kleman, J., Heyman, J., Fabel, D., Fredin, O., . . . Strömberg, B. (2016). Deglaciation of Fennoscandia. *Quaternary Science Reviews*, 91-121.

Söderberg, J., & Flodén, T. (1992). Gas seepages, gas eruptions and degassing structures in the seafloor along the Strömma tectonic lineament in the crystalline Stockholm Archipelago, east Sweden. *Continental Shelf Research*, 1157-1171.

Söderberg, P., & Flodén, T. (1997). Stratabound submarine terraces and pockmarks - indicators of spring sapping in glacial clay, Stockholm Archipelago, Sweden. *Proceedings of the Fourth Marine Geological Conference - The Baltic* (ss. 173-178). Uppsala: Sveriges Geologiska Undersökning.

Vardar, D., & Alpar, B. (2016). High-Resolution Seismic Characterization of Shallow Gas Accumulations in the Southern Shelf of Marmara Sea, Turkey. *Acta Geophysica*, 589-609.

Winterhalter, B., Flodén, T., Ignatius, H., Axberg, S., & Niemistö, L. (1981). The Baltic Sea. i W. Smith, & D. Barber, *Elsevier Oceanography Series Volume 30* (ss. 1-89). New York: Elsevier Scientific Publishing Company.

Zhang, J., & Satake, H. (2003). The chemical characteristics of submarine groundwater seepage in Toyama Bay, Central Japan. i M. Taniguchi, K. Wang, & T. Gamo, *Land and Marine Hydrogeology* (ss. 45-60). Amsterdam: Elsevier B.V.

# Appendix (I) SGU Maps

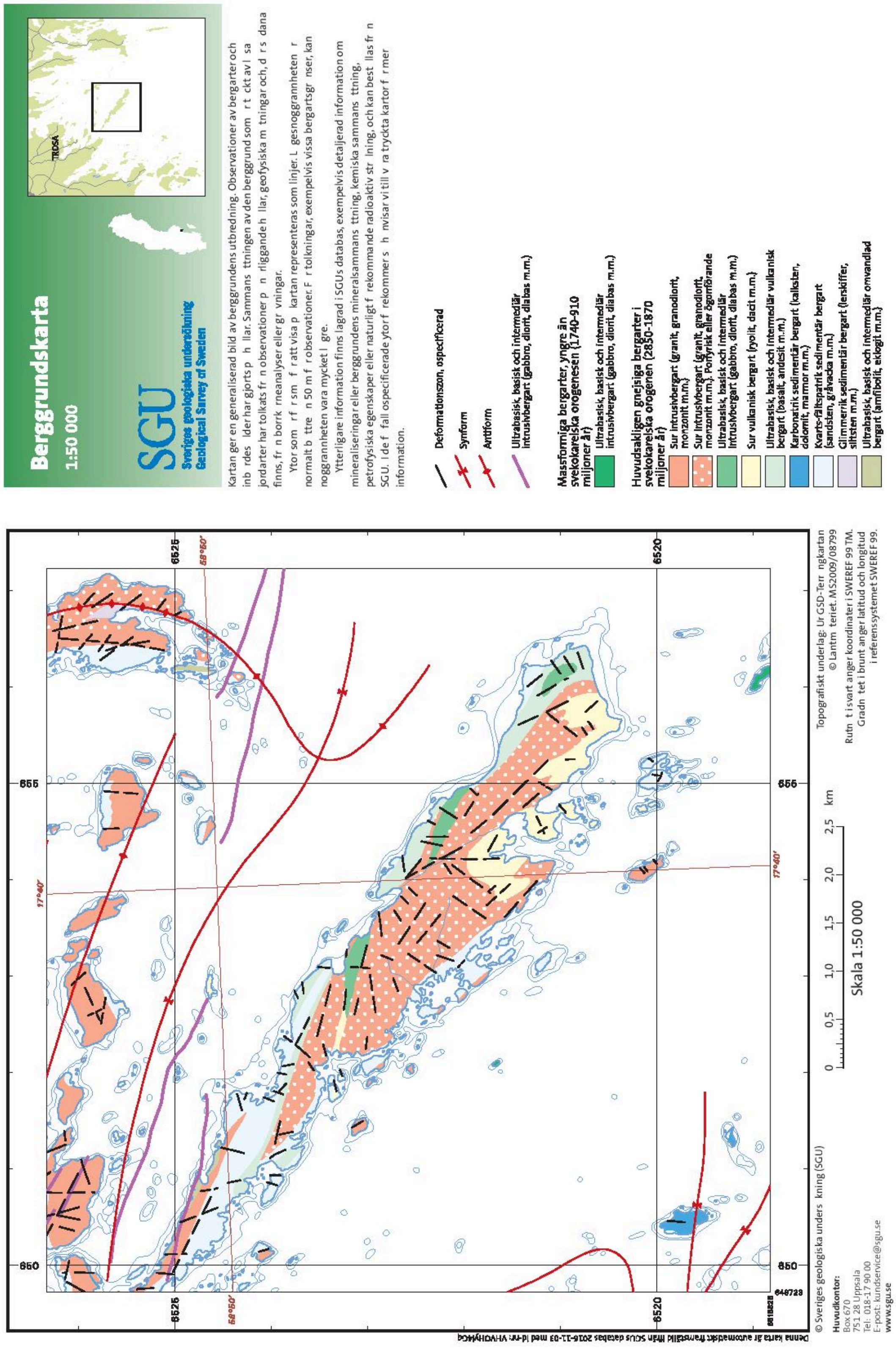

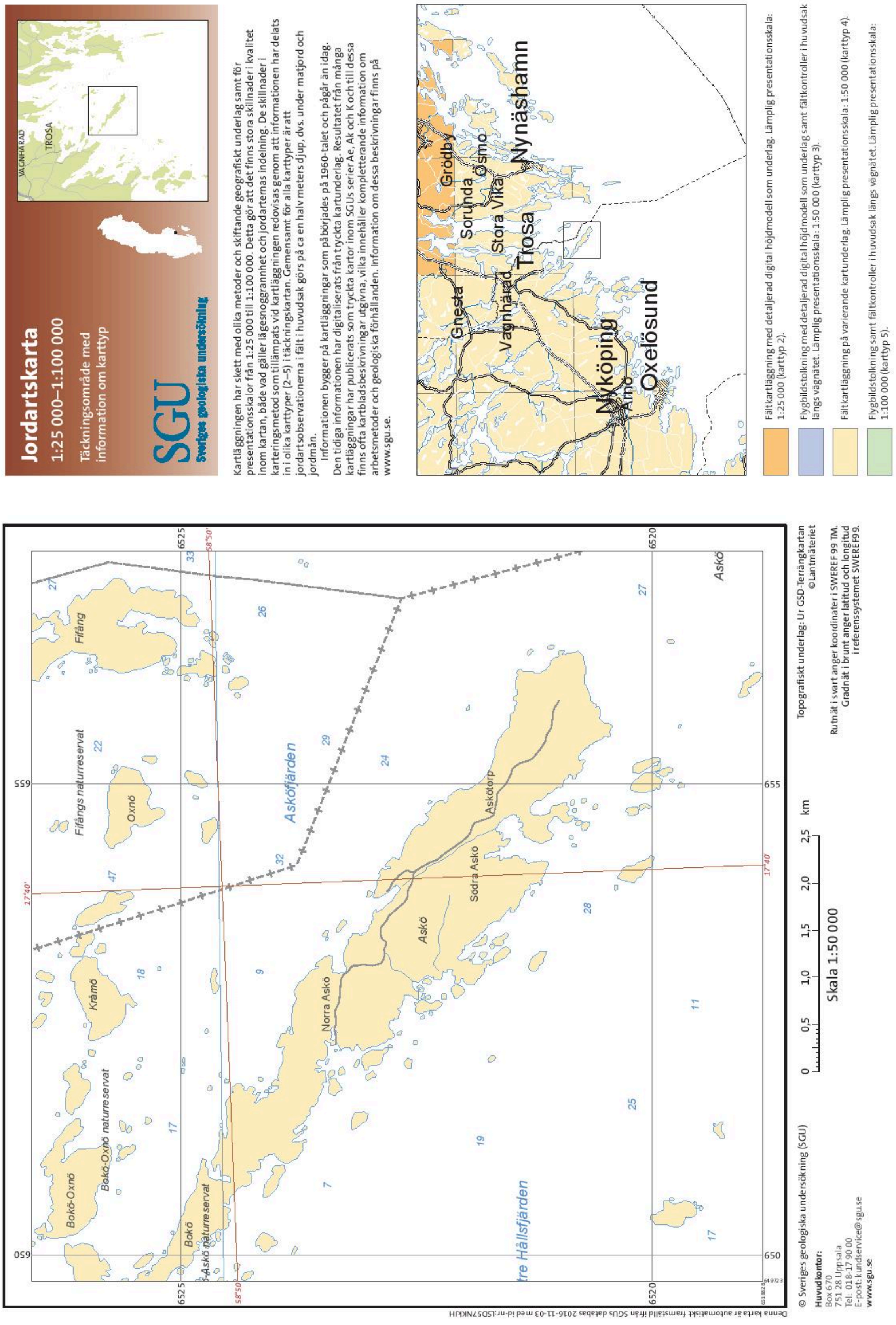
Jordartskarta
1:25 000–1:100 000
Täckningsområde med information om karttyp
SGU
Sveriges geologiska undersökning
VAGNHÄRAD
TROSA
Kartläggningen har skett med olika metoder och skiftande geografiskt underlag samt för presentationsskalor från 1:25 000 till 1:100 000. Detta gör att det finns stora skillnader i kvalitet inom kartan, både vad gäller lägesnoggrannhet och jordarternas indelning. De skillnader i karteringsmetod som tillämpats vid kartläggningen redovisas genom att informationen har delats in i olika karttyper (2–5) i täckningskartan. Gemensamt för alla karttyper är att jordartsobservationerna i fält i huvudsak görs på ca en halv meters djup, dvs. under matjord och jordmån.
Informationen bygger på kartläggningar som påbörjades på 1960-talet och pågår än idag. Den tidiga informationen har digitaliserats från tryckta kartunderlag. Resultatet från många kartläggningar har publicerats som tryckta kartor inom SGUs serier Ae, Ak och K och till dessa finns ofta kartbladsbeskrivningar utgivna, vilka innehåller kompletterande information om arbetsmetoder och geologiska förhållanden. Information om dessa beskrivningar finns på www.sgu.se.
Gnesta
Grödby
Sorunda
Ösmo
Vagnhärad
Stora Vika
Trosa
Nynäshamn
Nyköping
Arnö
Oxelösund
Fältkartläggning med detaljerad digital höjdmodell som underlag. Lämplig presentationsskala: 1:25 000 (karttyp 2).
Flygbildstolkning med detaljerad digital höjdmodell som underlag samt fältkontroller i huvudsak längs vägnätet. Lämplig presentationsskala: 1:50 000 (karttyp 3).
Fältkartläggning på varierande kartunderlag. Lämplig presentationsskala: 1:50 000 (karttyp 4).
Flygbildstolkning samt fältkontroller i huvudsak längs vägnätet. Lämplig presentationsskala: 1:100 000 (karttyp 5).
Bokö-Oxnö
Bokö-Oxnö naturreservat
Krämö
Fifångs naturreservat
Fifång
Oxnö
Bokö
Askö naturreservat
Asköfjärden
Norra Askö
Askö
Södra Askö
Asktorp
tre Hållsfjärden
6525
6520
650
655
17°40'
58°50'
© Sveriges geologiska undersökning (SGU)
Huvudkontor:
Box 670
751 28 Uppsala
Tel: 018-17 90 00
E-post: kundservice@sgu.se
www.sgu.se
0 0,5 1,0 1,5 2,0 2,5 km
Skala 1:50 000
Topografiskt underlag: Ur GSD-Terrängkartan ©Lantmäteriet
Rutnät i svart anger koordinater i SWEREF 99 TM. Gradnät i brunt anger latitud och longitud i referenssystemet SWEREF99.
Denna karta är automatiskt framställd ifrån SGUs databas 2016-11-03 med id-nr:LSDS7NKkJH

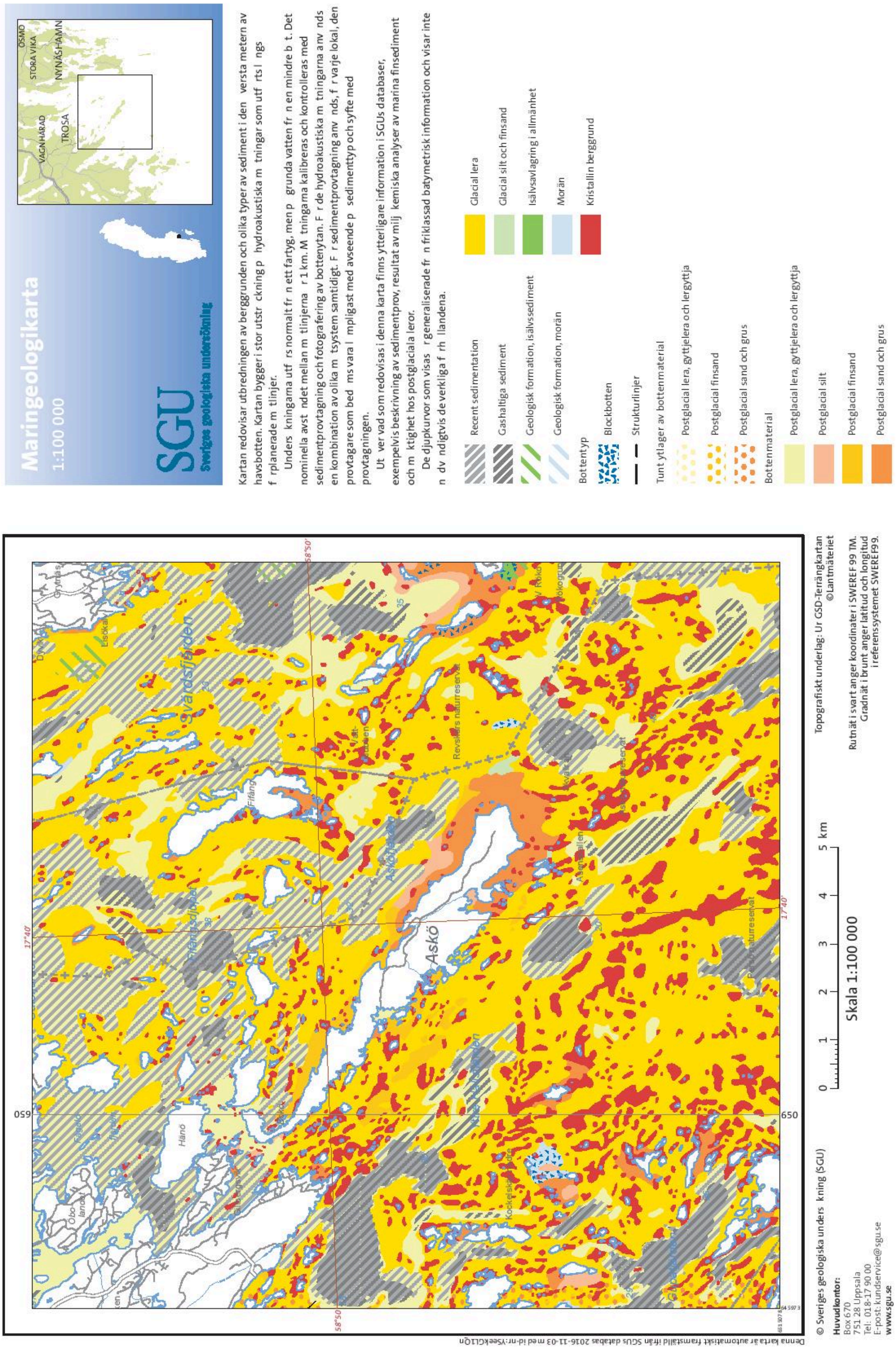
Maringeologikarta
1:100 000
SGU
Sveriges geologiska undersökning
Recent sedimentation
Gashaltiga sediment
Geologisk formation, isälvssediment
Geologisk formation, morän
Bottentyp
Blockbotten
Strukturlinjer
Tunt ytlager av bottenmaterial
Postglacial lera, gyttjelera och lergyttja
Postglacial finsand
Postglacial sand och grus
Bottenmaterial
Postglacial silt
Glacial lera
Glacial silt och finsand
Isälvsavlagring i allmänhet
Morän
Kristallin berggrund
Askö
Skala 1:100 000
Topografiskt underlag: Ur GSD-Terrängkartan ©Lantmäteriet
© Sveriges geologiska undersökning (SGU)

## Appendix (II) Static Surface of Study Area

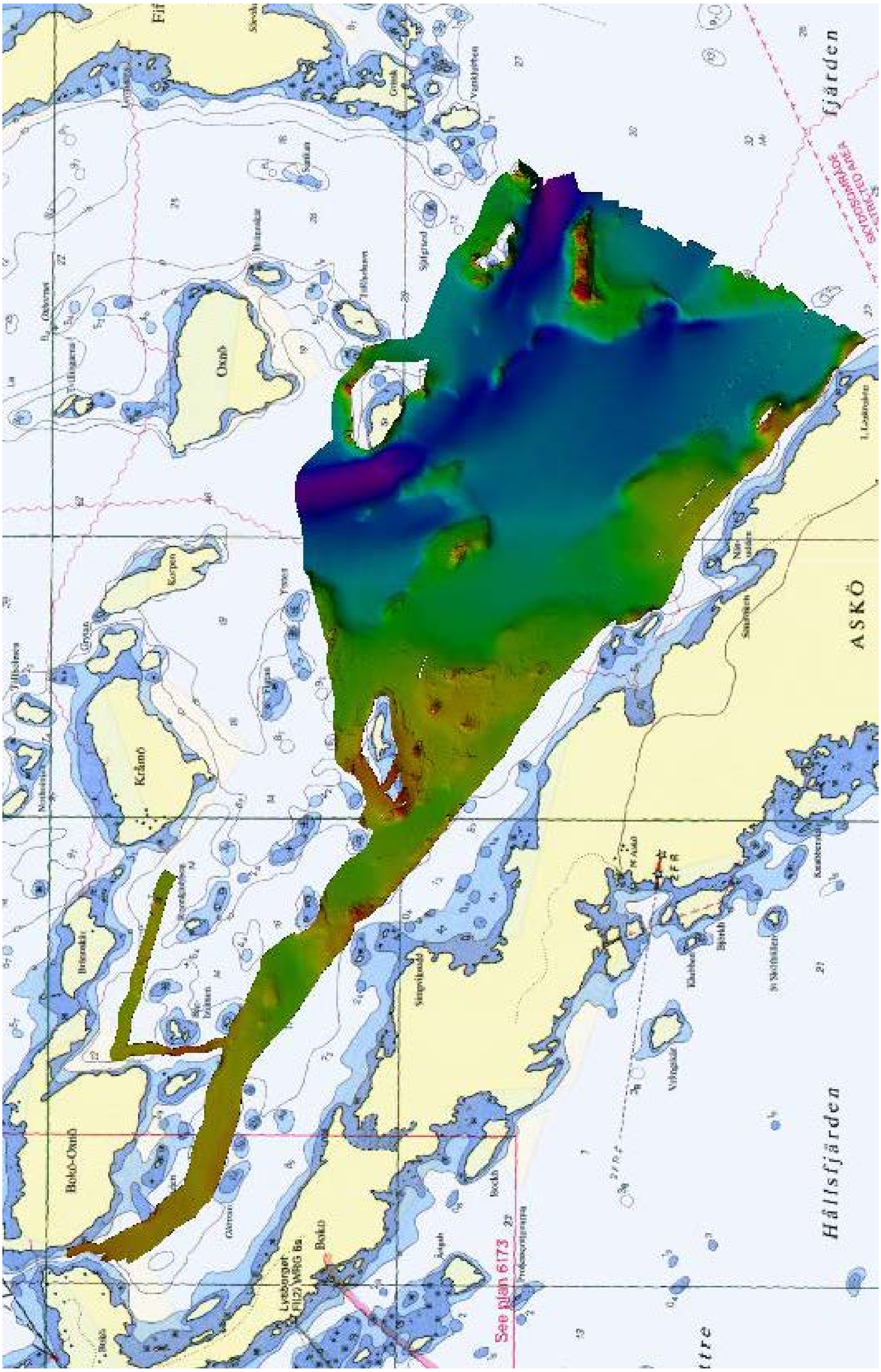

# Appendix (III) Original SBPs

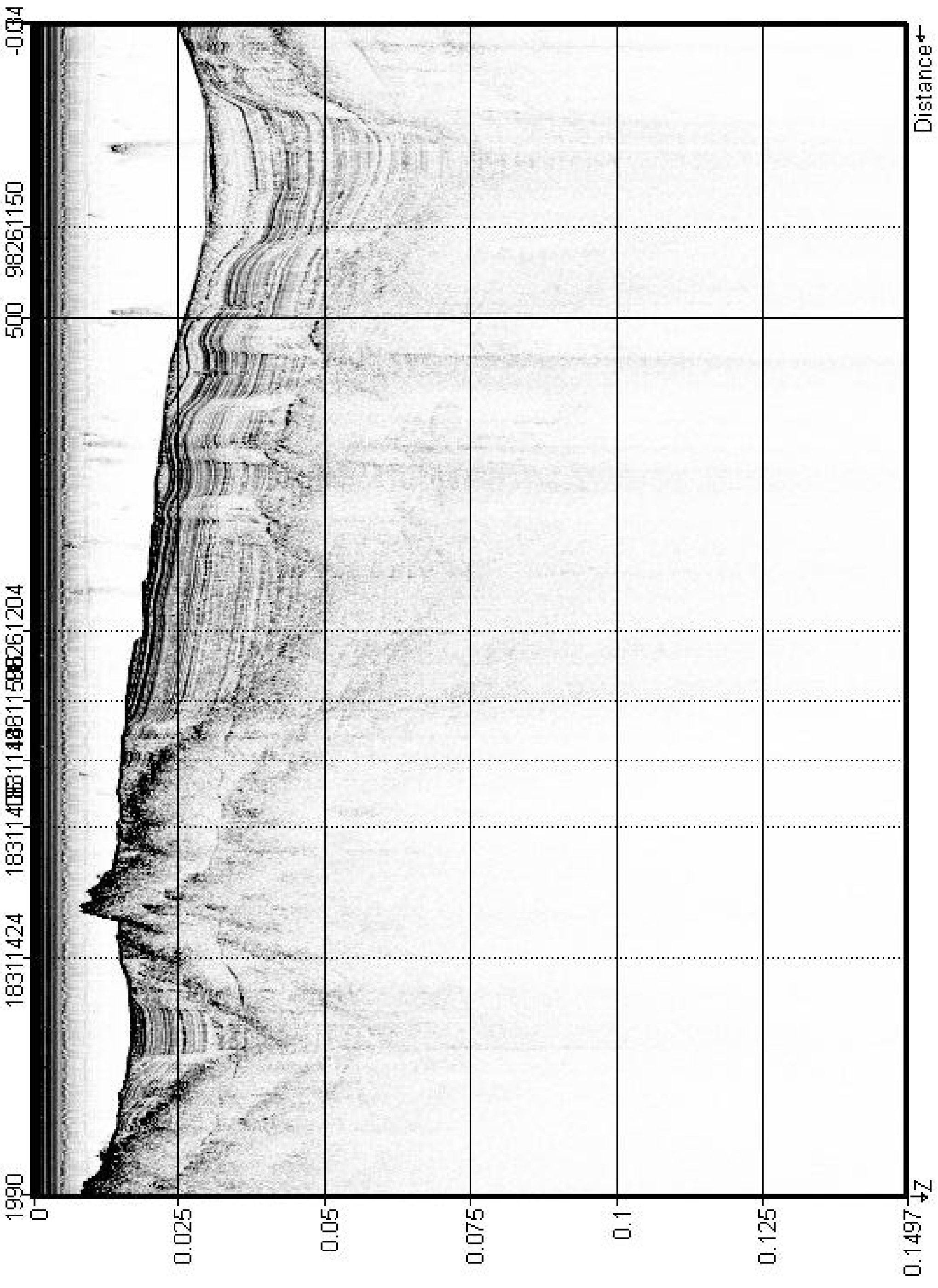

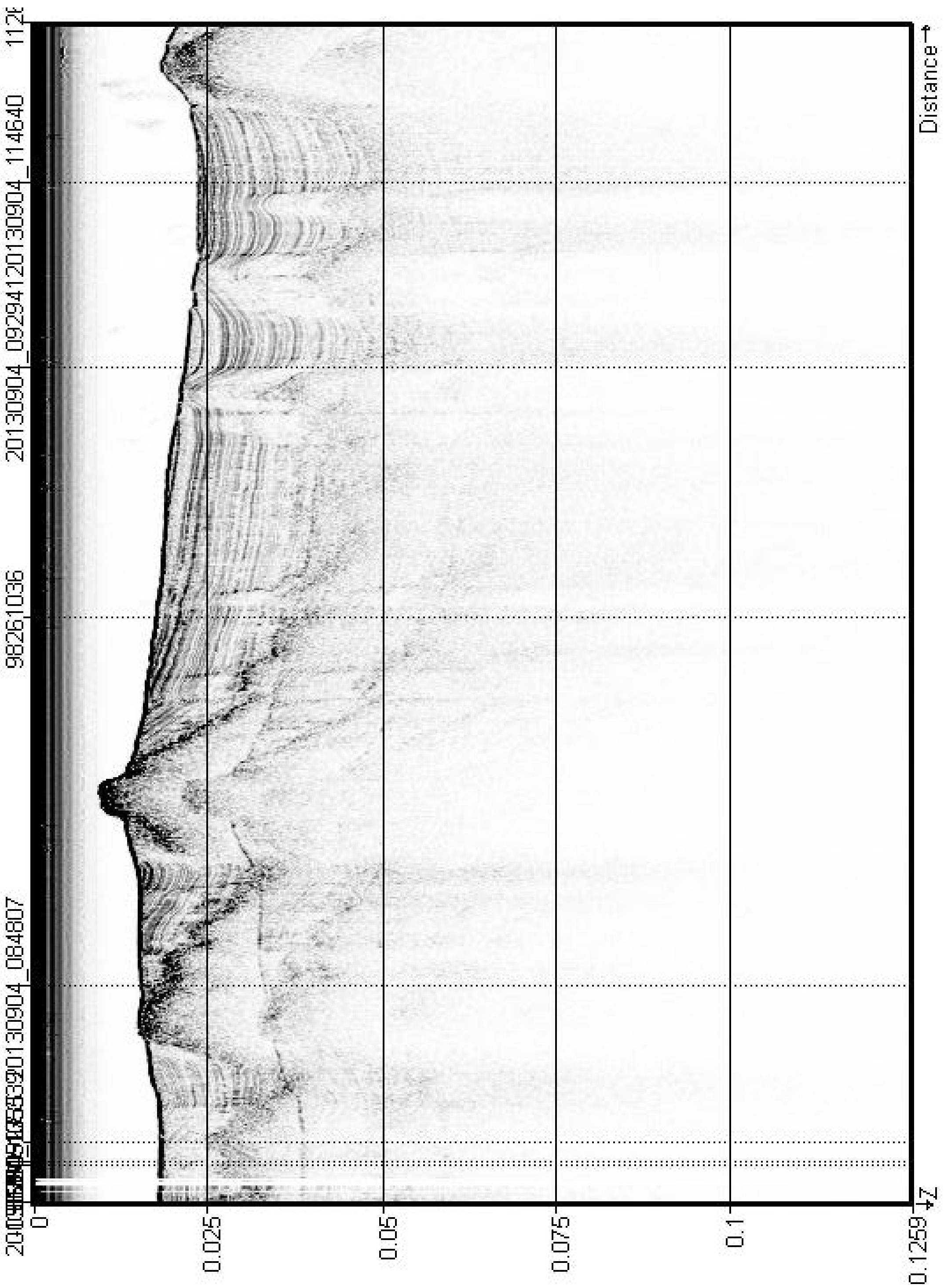

Distance
Z
0
0.025
0.05
0.075
0.1
0.1259
98261036
20130904_084807
20130904_092941
20130904_114640

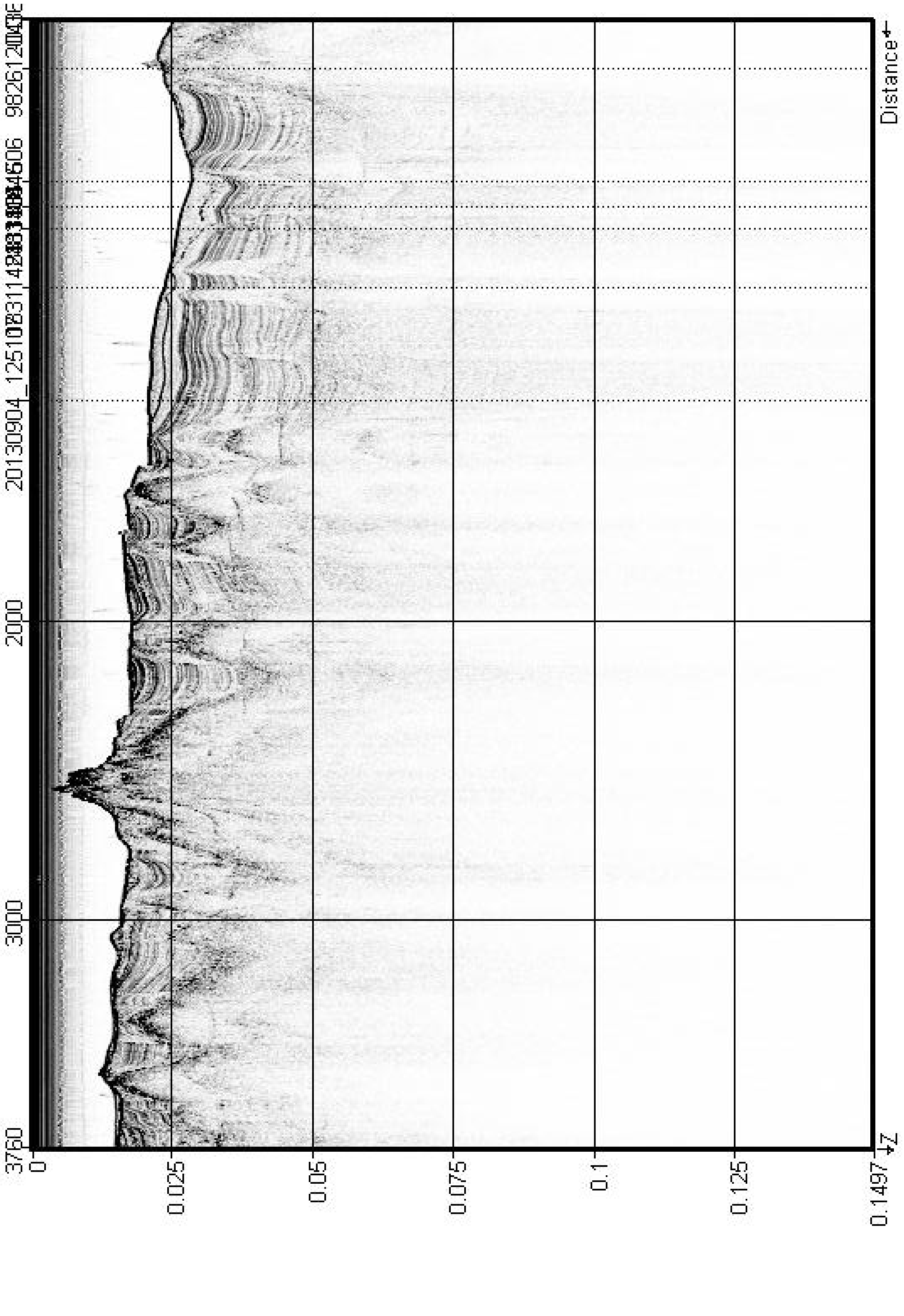
Distance
2000
3000
3760
0
0.025
0.05
0.075
0.1
0.125
0.1497
Z

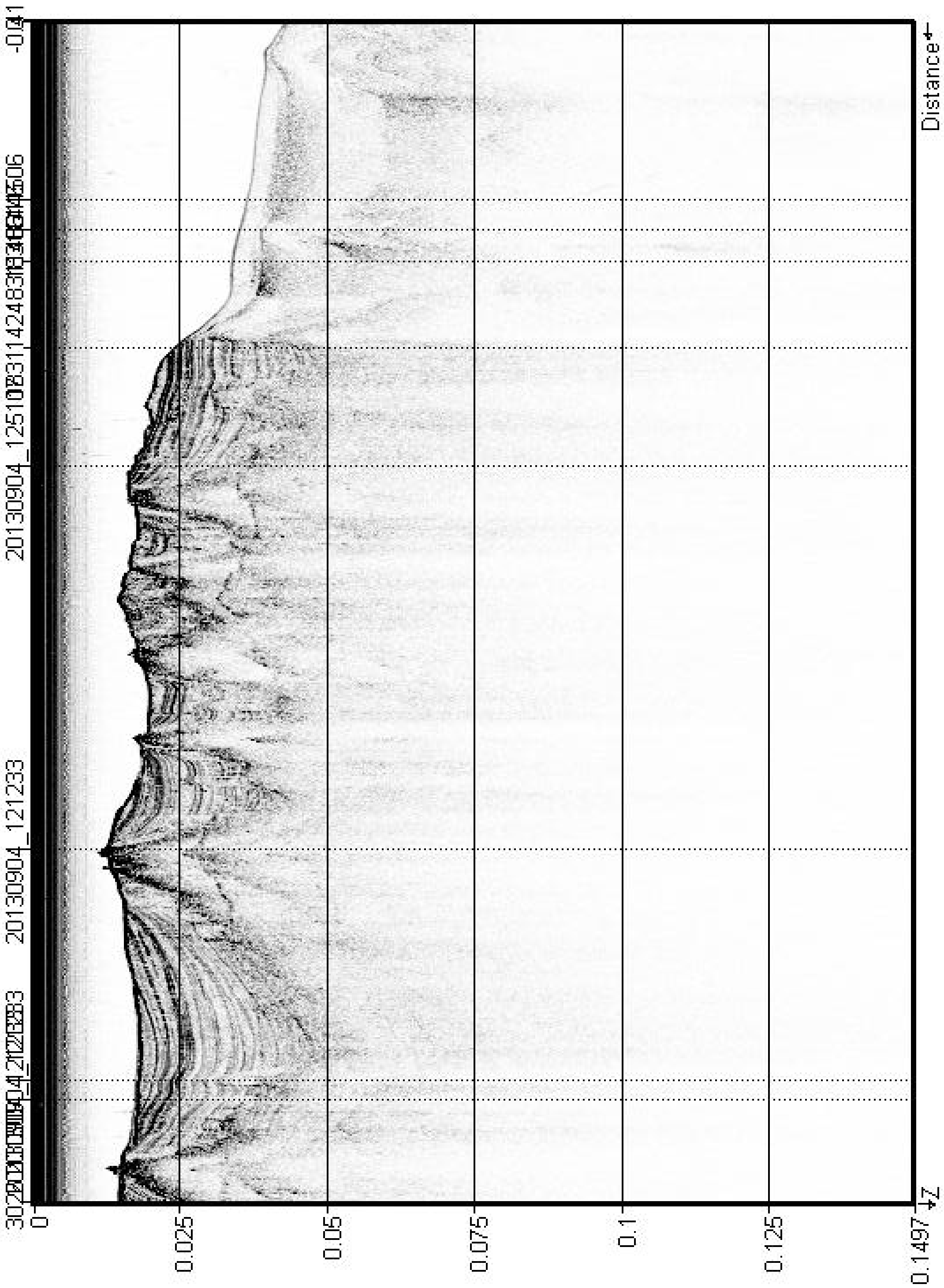
20130904_121233
20130904_125107
Distance
Z
0
0.025
0.05
0.075
0.1
0.125
0.1497

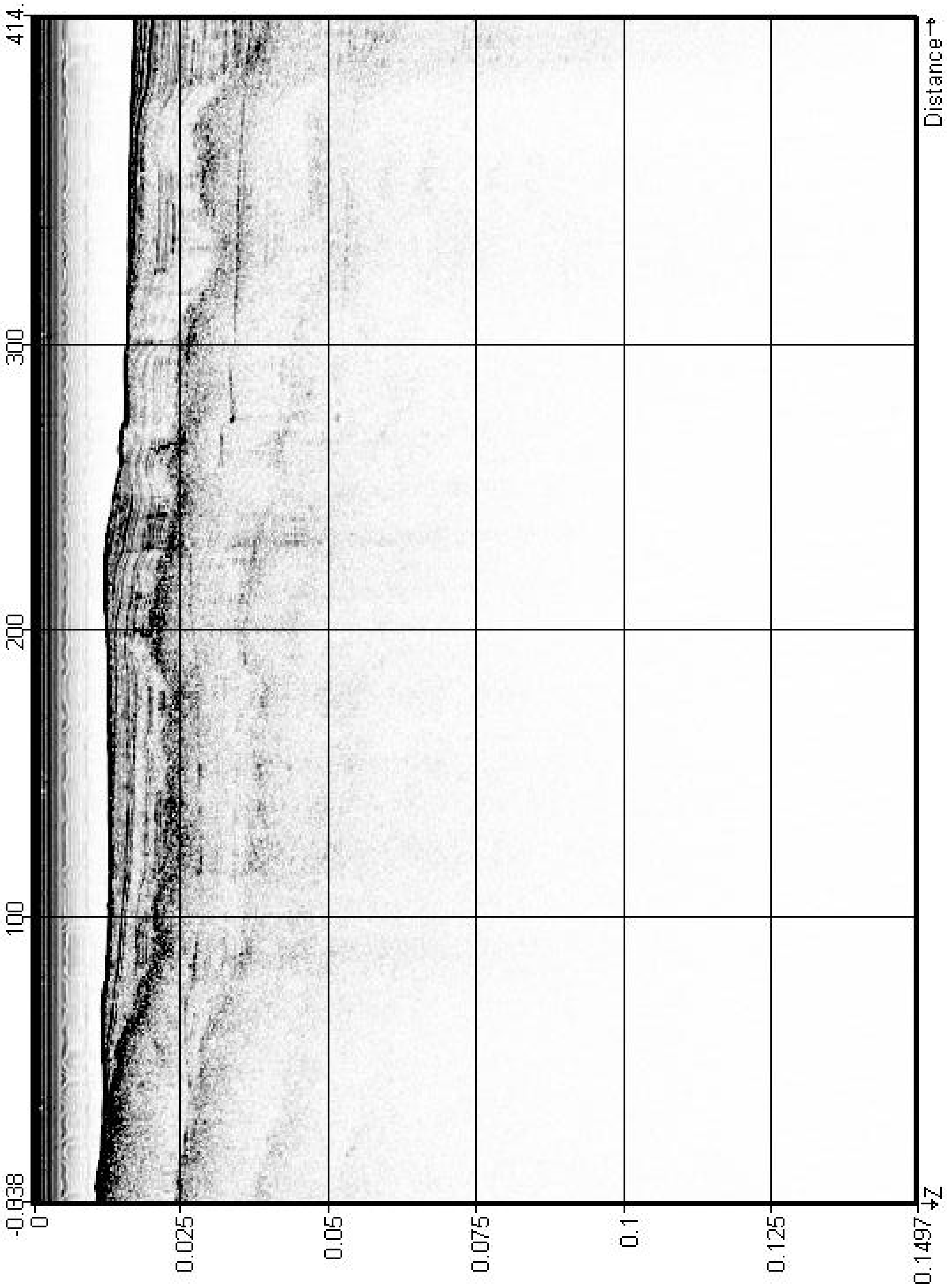
414.
300
200
100
-0.938
Distance
0
0.025
0.05
0.075
0.1
0.125
0.1497
Z

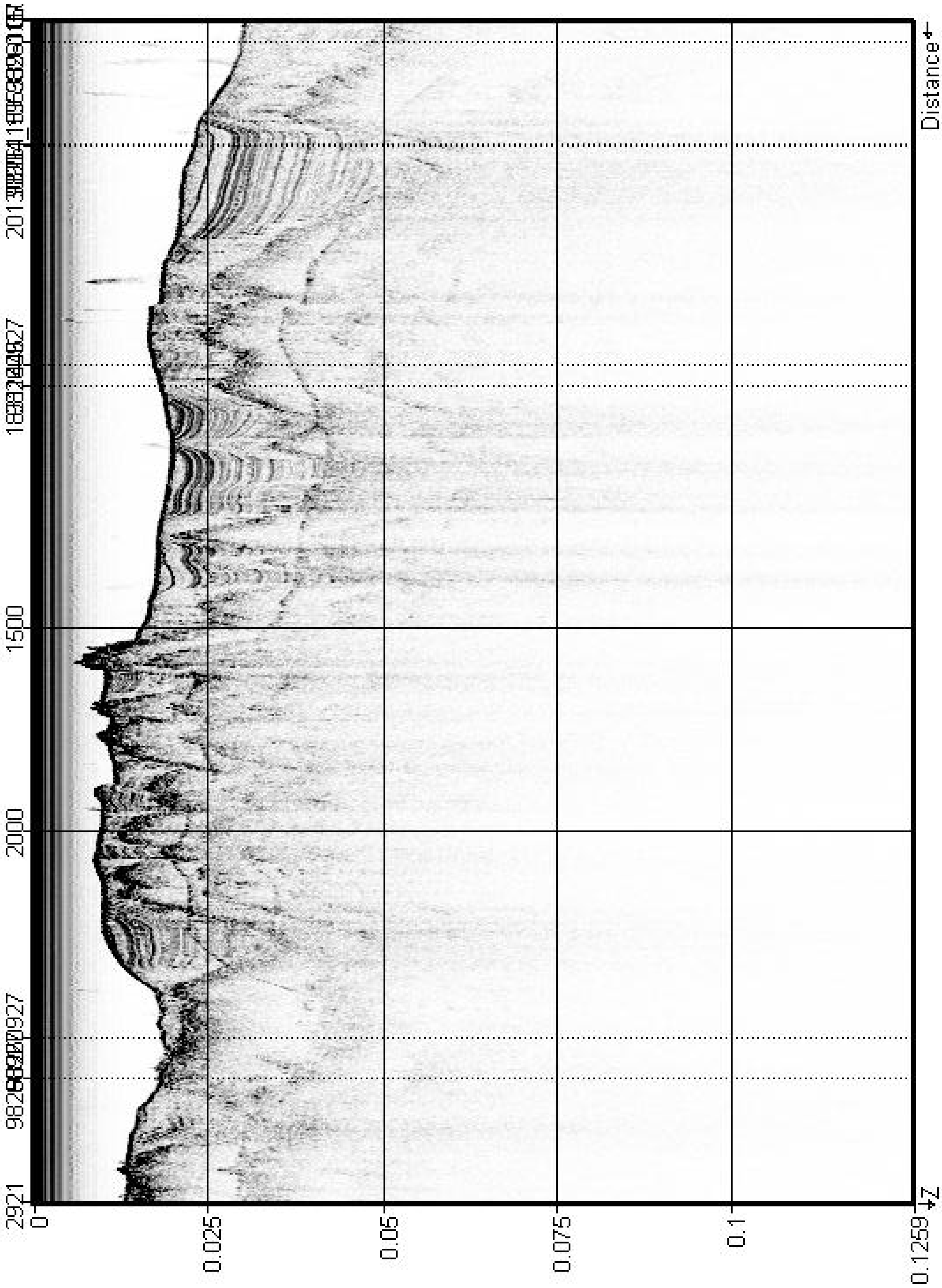
Distance
Z
0
0.025
0.05
0.075
0.1
0.1259
2921
1500
2000

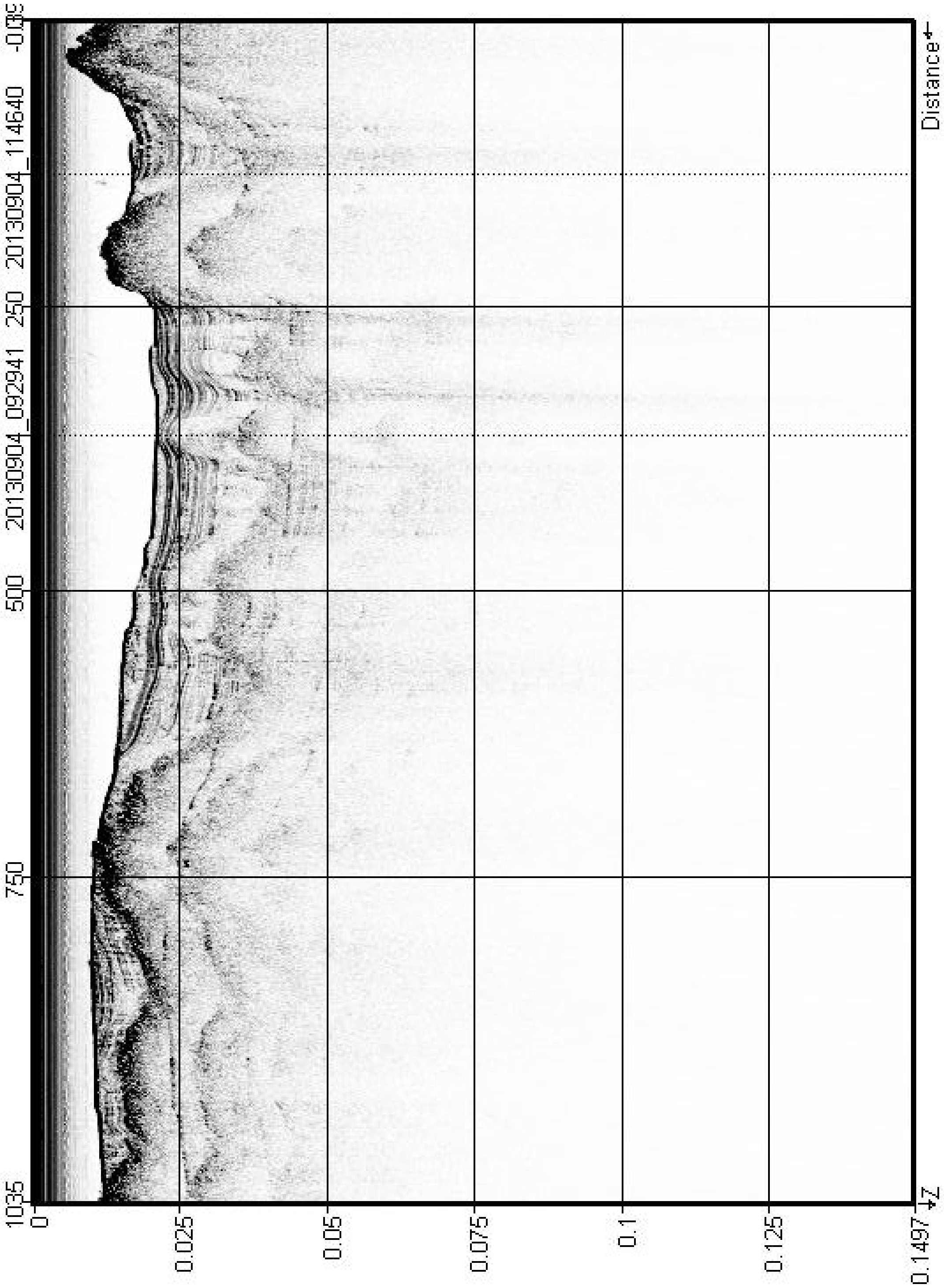
Distance
Z
20130904_114640
20130904_092941
250
500
750
1035
0
0.025
0.05
0.075
0.1
0.125
0.1497

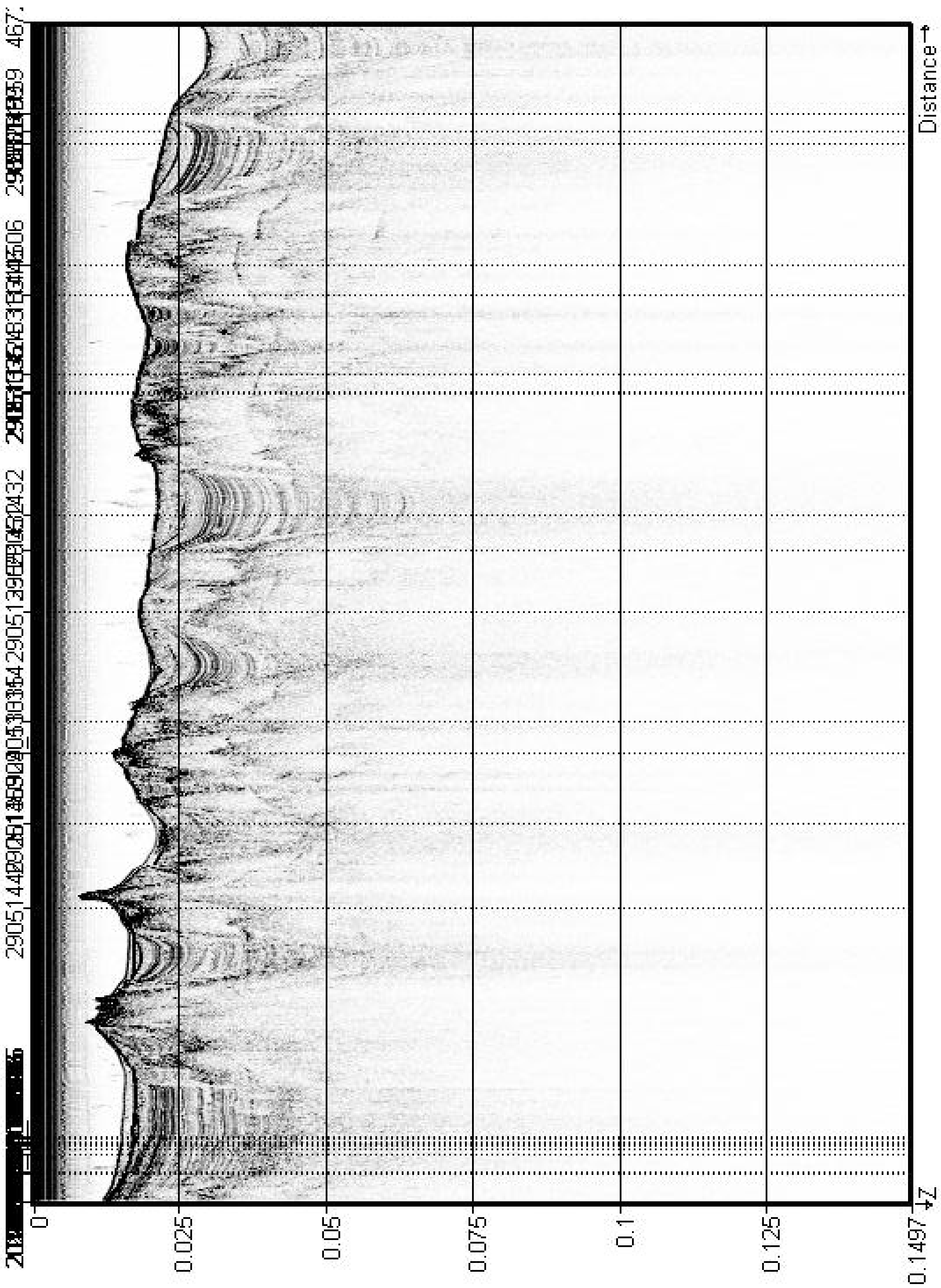
0
0.025
0.05
0.075
0.1
0.125
0.1497
Z
Distance